



MODEL COMPUTATION OF WATER CLUSTERING $(\text{H}_2\text{O})_n$ EFFECT IN THE NEGATIVE ION PROTON TRANSFER REACTIONS

By

GEMECHIS DEREJE DEGAGA

SUBMITTED IN PARTIAL FULFILLMENT OF THE
REQUIREMENTS FOR THE DEGREE OF
MASTER OF SCIENCE IN MATERIALS SCIENCE

AT

ADDIS ABABA UNIVERSITY
ADDIS ABABA, ETHIOPIA

JUNE 2010

ADDIS ABABA UNIVERSITY
DEPARTMENT OF
MATERIALS SCIENCE

Supervisor:

Dr. MULUGETA BEKELE

Examiners:

PROF. TEKETEL YOHANNES

Dr. AHMED MUSTEFA

ADDIS ABABA UNIVERSITY

Date: JUNE 2010

Author: **GEMECHIS DEREJE DEGAGA**

Title: Model Computation of Water Clustering (H₂O)_n effect in the Negative Ion Proton Transfer Reactions

Department: Materials Science

Degree: **M.Sc.** Convocation: **JUNE** Year: **2010**

Permission is herewith granted to Addis Ababa University to circulate and to have copied for non-commercial purposes, at its discretion, the above title upon the request of individuals or institutions.

Signature of Author

THE AUTHOR RESERVES OTHER PUBLICATION RIGHTS, AND NEITHER THE THESIS NOR EXTENSIVE EXTRACTS FROM IT MAY BE PRINTED OR OTHERWISE REPRODUCED WITHOUT THE AUTHOR'S WRITTEN PERMISSION

THE AUTHOR ATTESTS THAT PERMISSION HAS BEEN OBTAINED FOR THE USE OF ANY COPYRIGHTED MATERIAL APPEARING IN THIS THESIS (OTHER THAN BRIEF EXCERPTS REQUIRING ONLY PROPER ACKNOWLEDGEMENT IN SCHOLARLY WRITING) AND THAT ALL SUCH USES ARE CLEARLY ACKNOWLEDGED

For those family and friends of mine who have
unlimited potential but cannot attend the school.

Table of Contents

LIST OF TABLES	I
LIST OF FIGURES	II
ABSTRACT	III
ACKNOWLEDGEMENTS	IV
CHAPTER ONE	1
INTRODUCTION	1
CHAPTER TWO	5
OBJECTIVE	5
2.1. GENERAL OBJECTIVE	5
2.2. SPECIFIC OBJECTIVES	5
CHAPTER THREE	7
THEORETICAL BACKGROUNDS	7
3.1 PROTON TRANSFER REACTION MASS SPECTROMETER	7
3.2 ION-NEUTRAL REACTION KINETICS	9
3.3 GAS PHASE ION THERMOCHEMISTRY	22
CHAPTER FOUR	25
METHODOLOGY	25
CHAPTER FIVE	27
RESULTS AND DISCUSSION	27
5.1. REVIEW OF RELATED WORKS	27
5.2. COMPARISON OF OUR COMPUTATIONAL RESULTS WITH LITERATURE	29
5.3. THE EFFECT OF WATER CLUSTERING ON THE REACTION RATE CONSTANT OF ACETATE ION WITH ACETIC AND FORMIC ACID	29
5.4. THE STUDY OF THE EFFECT OF MOLECULAR SIZE AND STRUCTURE ON THE MAGNITUDE OF REACTION RATE CONSTANT	32
5.5. COMPARISON OF RATE CONSTANT OF SOME THE ENVIRONMENTALLY IMPORTANT MOLECULES WITH BARE AND CLUSTERED/HYDRATED ACETATE ION	34
5.6. THERMODYNAMIC EFFECT OF WATER CLUSTERING IN THE NEGATIVE ION PROTON TRANSFER REACTION (NI-PTR)	35
CHAPTER SIX	39
CONCLUSION	39
Appendix	
Reference	

List of tables

5.1: Comparison of ADO to the Lengevin, locked dipole and the experiment	28
5.2: comparison of our computational results to the available literature.....	29
5.3: The input data.....	30
5.4: the polarizability α (in the cube of Angstrom), dipole moment μ_D (in Debye), density (in g/cm^3) and molecular mass (in amu) of the alkali chlorides.....	32
6.5: the polarizability α (in the cube of Angstrom), dipole moment μ_D (in Debye), density ρ (in g/cm^3) and molecular mass (in amu) of the molecules.....	34

List of figures

3.1: the program skeleton.....	8
3.2: The main steps in mass spectrometer and the three modules.....	9
3.3: a rough sketch of NI-PTRM mass spectrometry.....	13
3.4: reaction coordinates for the reaction between HO ⁻ and CH ₃ Br.....	15
3.5: Ion-neutral molecule trajectory.....	17
3.6: The point charge and the point dipole interaction orientation.....	21
4.1: (curtsey of G. Kummerlöwe and M. Beyer, Int. J. of Mass Spec, 244 (1) p84 - 90, 2005)	26
5.1: reaction rate constant for the reaction $(H_2O)_n^- + CO_2 \rightarrow CO_2(H_2O)_{n-m}^- + mH_2O$ computed using HAS (dot-dashed), ADO (dotted) and the purely geometric K _g (dashed) models.....	28
5.2: Rate constant as function of cluster size for acetic acid.....	30
5.3: Rate constant as function of cluster size for formic acid.....	31
5.4: reduced mass as function of cluster size for HAS theory.....	31
5.5: Proton transfer rate constant from alkyl chlorides, listed along the horizontal axis, to acetate ion computed by using HAS and ADO theory.....	33
5.6: Clustering effect on the rate constant in the case of ADO theory.....	35
5.7: Clustering effect on the rate constant in the case of HSA theory.....	36
5.8: cluttering effect on Gibbs free energy change in the case of ADO theory.....	37
5.9: cluttering effect on Gibbs free energy change in the case of HSA theory.....	38

Abstract

We report the effect of water clustering $(\text{H}_2\text{O})_n$ in the negative ion proton transfer reactions on reaction rate constants and the change in the Gibbs free energy of the corresponding reactions. Reaction rate constant of the reaction between the new proposed reagent acetate ion CH_3COO^- than the usual hydronium H_3O^+ and environmentally important molecules were computed. The computation was made using the hard sphere average dipole orientation theory (HSA) and the average dipole orientation theory (ADO) as an investigation tool. It was found that rate constant decreases for a range of cluster size and starts to below up steadily for the HSA. For ADO, it decreases approaching a lower limiting value. Rate constant were observed to rise as molecular size in enlarges and became non-sensitive to isomers of the same molecule for molecules which have similar dipole moments but different molecular size and structural configuration. Fifteen atmospherically potential molecules were chosen in the study scheme of the effect of the clustering to the reagent ion on the proton transfer reaction rate constant and the change in Gibbs free energy of these reactions. In both cases of the theories, the computed results of the rate constants of the clustered reagent ion were found to be less than that of the non-clustered. In contrary to this, change in the Gibbs free energy of the reactions was found to be greater. The rate constant of the reaction between clustered ions of these molecules and the neutral acetic acid molecule was also computed. These computed results facilitate the use of NI-PTR MS technique, which uses acetate ion as reagent ion, in the application of laboratory investigations and field measurement of environmentally important volatile organic compounds VOCs.

Acknowledgements

Above all, I would like to thank the almighty; God, for letting me accomplish this stage.

I am deeply indebted Dr. Mulugeta Bekele, my advisor, for his valuable suggestions and constant support and friendly approach during this thesis works. His tireless follow up and his consistent support will be in my memory forever. To gather with him, I would like to thank all his collaborators; Mr. A.K. Cochran, Dr. Solomon Bililign, Dr. M. Fiddler, and their group for their unlimited materials and data supply and fruit full guide lines.

My strongest thank is addressed to my Family and my Friends who helped me in any respects. They are the hero of my success. My honorable thank goes to Mr. Debala Mosisa for his special support.

I have derived materials from many research journals and books, and I would like to forward my grateful thank to the authors of those publications and books too.

Chapter one

Introduction

In gas-phase ion chemistry, the collision rate between the ion and a neutral reactant forms the upper theoretical limit for the reaction rate constant. This rate is frequently calculated with the help of average dipole orientation (ADO) theory [1].

$$K_{ADO} = \left(\frac{2\pi Q}{\mu^{1/2}} \right) \left[\alpha^{1/2} + C\mu_D \left(\frac{2}{\pi k_B T} \right)^{1/2} \right] \quad (1.0.1)$$

ADO theory is based on the classical trajectory of a linear dipole in the field of a point charge, which is the standard approach for the theoretical investigation of capture processes.

Measured reaction rate constants of ionic clusters often exceed the collision rate calculated with the widely used Average Dipole Orientation (ADO) theory [2]. The attraction between the point charge and the neutral molecule is described with the interaction potential from ADO theory but is not sufficient for the clustering case. HSA is a simple and universally applicable model to estimate these collision rates. In the HSA model, the charge of an ion cluster is concentrated at the center. The cluster and the neutral reaction partner are treated as hard spheres and the charge is treated as a point charge. For weakly polarizable clusters such as $(\text{H}_2\text{O})_n^-$, the newly derived HSA rate constants lie close to experimentally measured rate constants.

$$k_{HSA} = \int_0^{v_c} k_{ADO}(v) f(v) dv + \int_{v_c}^{\infty} k_{HSD}(v) f(v) dv \quad (1.0.2)$$

$$f(v) = 4\pi v^2 \left(\frac{\mu}{2\pi k_B T} \right)^{2/3} e^{-\frac{\mu v^2}{2\pi k_B T}}$$

where $K_{ADO}(v) = \frac{q}{2\varepsilon_0\sqrt{\mu}} \left(\sqrt{\alpha} + \frac{c\mu_D}{\sqrt{\mu}v} \right)$, $k_{HSD}(v) = \pi v b_g^2 + \frac{\alpha q^2}{16\pi^2 \varepsilon_0^2 \mu v b_g^2} + \frac{c\mu_D q}{2\pi \varepsilon_0 \mu v}$,

and $v_c = \sqrt{\frac{\alpha q^2}{16\pi^2 \varepsilon_0^2 \mu b_g^4}}$

Here, μ is the reduced mass of the molecule and the cluster, v their relative velocity, b the impact parameter, r the distance between the center of the cluster and the center of the molecule, q the cluster charge, and ε_0 the vacuum permittivity. The neutral

molecule is described by its polarizability α , its dipole moment μ_D and the dipole locking constant c .

Gas phase acidity of a molecule AH, $\Delta_{\text{acid}}G$ (AH), is the Gibbs free energy change of the reaction [3]

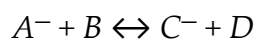


The basis of this technique is selective ionization of acidic species through the transfer of a proton to the conjugate anion of a weaker acid and the subsequent detection of A^- via mass spectrometry;



The ionization scheme requires that the analyte be a stronger gas phase acid than the acidic form of the reagent ion.

Acidity determinations are based on equilibrium constants for ion/molecule reactions:



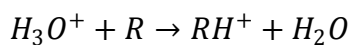
since the equilibrium constant,

$$K_{eq} = [\text{C}^-][\text{D}] / [\text{A}^-][\text{B}] \quad (1.0.3)$$

directly gives a value for the gibbs free energy change associated with the reaction

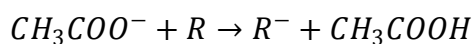
$$RT \ln K_{eq} = \Delta G = \Delta H - T \Delta S. \quad (1.0.4)$$

The prime concern of this work is the investigation of effect of water clustering in the negative ion proton transfer reactions on their rate constant and Gibbs free energy. Such reaction types are the one that used in negative ion proton transfer reaction mass spectrometer (NI-PTR MS) for the ionization mechanism of the molecule under analysis, the analyte. Hydronium ion H_3O^+ is the common reagent ion used in proton transfer reaction mass spectrometer PTR MS. The reaction associated to such instrument is given by



where R is the molecule under analysis [4].

Here we propose acetate ion CH_3COO^- as new reagent ion as it is very selective, not depleted by other trace gases, and because of its higher proton affinity PA than volatile organic molecules [5]. The corresponding reaction represents the ionization method in the case of NI-PTR MS is as follow



Negative Ion Proton Transfer Mass Spectrometry (NI-PTRMS)) is among the recently developed instrumental technique in both kinetic and thermodynamic measurement of the gas-phase acidic gases. One of the more useful applications of PTRMS-NI will be the measurement of carboxylic acids in the gas or particle phase. The research proposed here is generally the study of the effect of water $[(H_2O)_n]$ clustering in Negative Ion Proton Transfer reaction Mass Spectrometer (NI-PTRMS) in Time-of-Flight system for the measurement of Trace Gases in Troposphere. The research focuses on the study of the clustering effect on the important kinetic and thermodynamic variables of gas phase carboxylic acids [5].

This work has broad impacts in two areas: Air quality and Climate. The carboxylic acids to be studied in this work are connected to these areas, the carbon cycle, because carboxylic acids are key players in organic aerosol chemistry. Climate systems are highly varying, changing in hours, days or years. Many physical, chemical and biological interactions occur among the various components of the climate system on a wide range of space and time scales, making the system extremely complex. Although the components of the climate system are very different in their composition, they are interrelated by physical and chemical properties and by their structure and behavior. Understanding the chemistry of volatile organic compounds (VOCs) will contribute to the understanding of a major social problem: Climate change.

VOCs (Volatile organic compounds) in the atmosphere are emitted in large quantities from variety of different natural and anthropogenic sources. VOCs are key participants in the formation of ozone and aerosols and they play a significant role in determining regional air quality, chemistry of the global troposphere and global carbon cycle.

Carboxylic acids, RC(O)OH , play a central role in the VOC chemistry of the troposphere. They are key intermediate species in the photooxidation of organic compounds and undergo interesting and important chemistry in both the gas and particle phases. Sources of small carboxylic acids include plant and soil biogenic sources, gas phase chemistry involving; O_3 -alkene chemistry, $\text{RC(O)OO} + \text{HO}_2$ chemistry, $\text{RC(O)OO} +$ aqueous droplets, and particle phase oxidation of organic compounds involving OH and O_3 [6].

We are interested in this work because, the computed results of this work will be helpful to the complementary task done by experimentalists who use acetate ion as a reagent ion in NI-PTR MS for the determination of $\text{P}H$, $\text{p}K_a$ and other variables associated to the atmospherically important molecules in the troposphere. Beyond this it provides useful information about clustering effect of water on reaction rate constants and change in Gibbs free energy in laboratory and field application of such instruments.

The rest of the chapters are organized in such a way that; chapter two informs the objective of this work, chapter three builds up the body talking about NI-PTR MS, ion-neutral reaction kinetics and gas phase ion thermochemistry to endow with general information. Chapter four discusses the methodology used. Important review literature and results and discussion are made under chapter five. Finally conclusions are presented in chapter six.

Chapter two

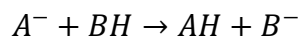
Objective

2.1. General objective

The general objective of the research is to study the effect of $[(H_2O)_n]$ clustering using computer simulation in Negative Ion Proton Transfer reactions. We apply hard sphere average dipole orientation theory (HSA) and average dipole orientation theory (ADO) for our study of the effect. The measurements include effect of the clustering on reaction rate constant and the change in Gibbs free energy of the reaction.

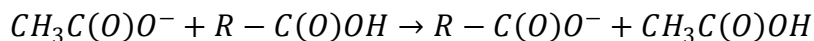
2.2. Specific objectives

- 1) The research includes a number of specific objectives needed to be attained at the end. The effect of the clustering on the rate constant will be computed using both theories for proton transfer reaction (PTR) of the kind

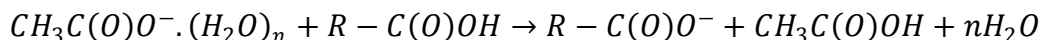


where $A^- = CH_3C(O)O^-$ and $B = R - C(O)O$, $R = H, C_nH_{2n+1}$, $n = 1, 2, 3, \dots$

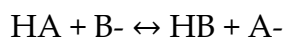
or this can be rewritten as



The corresponding reaction to study the effect then becomes



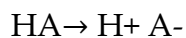
- 2) Molecular size and structural configuration are tested for their effect on proton transfer reaction rate constants. In this test we choose eight alkyl chlorides which have similar dipole moments but different molecular size and structural configuration.
- 3) The gas phase acidities of species of interest will be computed by determining relative ion densities at the exit of the flow tube, as a function of the neutral concentration. The reaction of an acidic compound with the conjugate anion of another acid sets up equilibrium of the following reaction type



The associated equilibrium constant, $K_{eq} = [A^-][HB]/[B^-][HA]$, can then be related to the ΔG for the reaction;

$$\Delta G = -RT \ln K_{eq}. \quad (2.0.1)$$

The gas phase acidity of a species, HA, is defined as ΔG for the process



Using this fact we have selected fifteen environmentally potential molecules in such a way that molecules of wide range of dipole moments and polarizability constants are considered to study the effect on the rate constant and hence the change in Gibbs free energy. The relative gas phase acidities determined in the proposed computation can be put on an absolute scale using well established literature values for one or more acids, e.g. acetic acid.

Chapter three

Theoretical backgrounds

3.1 Proton transfer reaction mass spectrometer

Mass spectrometry (MS) is an analytical technique for the determination of the elemental composition of a sample molecule. It is also used for elucidating the chemical structures of molecules, such as peptides and other chemical compounds. The MS principle consists of ionizing chemical compounds to generate charged molecules or molecule fragments and measurement of their mass-to-charge ratios. In a typical MS procedure the following five steps [7]:

- 1) A sample is loaded onto the MS instrument
- 2) The components of the sample are ionized by one of a variety of methods which results in the formation of charged particles
- 3) Directing the ions into an electric and/or magnetic field
- 4) computation of the mass-to-charge ratio of the particles based on the details of motion of the ions as they transit through electromagnetic fields
- 5) Detection of the ions, which in step 4 were sorted according to m/z .

MS instruments consist of three modules, Fig 3.1: an ion source, which can convert gas phase sample molecules into ions (or, in the case of electrospray ionization, move ions that exist in solution into the gas phase); a mass analyzer, which sorts the ions by their masses by applying electromagnetic fields; and a detector, which measures the value of an indicator quantity and thus provides data for calculating the abundances of each ion present. The technique has both qualitative and quantitative uses. These include identifying unknown compounds, determining the isotopic composition of elements in a molecule, and determining the structure of a compound by observing its fragmentation. Other uses include quantifying the amount of a compound in a sample or studying the fundamentals of gas phase ion chemistry (the chemistry of ions and neutrals in a vacuum). MS is now in very common use in analytical laboratories that study physical, chemical, or biological properties of a great variety of compounds.

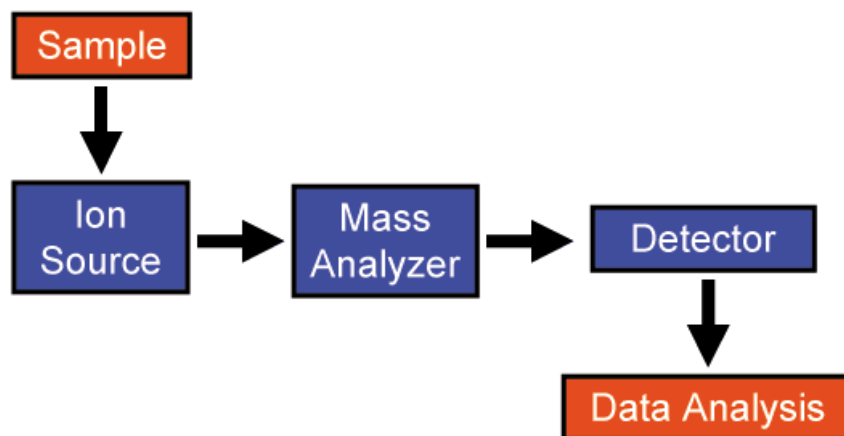


Figure 3.1: The main steps in mass spectrometer and the three modules.

Over the last decade the PTR-MS technique has been used extensively in environmental sciences as a fast VOC sensor. PTR-MS uses proton transfer reactions to chemically ionize volatile organic compounds (VOCs) present in gaseous media e.g. in air. With this technique, a variety of organic species in complex matrices can be monitored on-line with detection limits as low as a few pptv. The photo-oxidation of VOC leads to ozone and aerosol formation, which are both major air pollutants. They have adverse effects on health, and are significant factors for the Earth climate [8, 9].

The fundamental difference between a conventional MS and PTR-MS is the “soft ionization” method used to ionize the organic molecules. PTR-MS uses chemical ionization, in which the VOC molecules react with charged ions, in this case hydroxonium ions (H_3O^+) produced in an external ion source. H_3O^+ primary ions enter the drift tube (DT), which is flushed continuously with ambient air, and undergo non-reactive collisions with any of the common components in air (N_2 , O_2 , Ar, CO_2 , ..). H_3O^+ ions transfer their proton exclusively to VOC molecules that have proton affinities higher than that of water, making the reaction:



and forming VOCH^+ ions with a collision efficiency of unity.

The density of product ions [VOCH^+] in the DT follow pseudo first-order kinetics as expressed in the following equation, where t is the average reaction time the ions spend in the DT, and k is the reaction rate constant.

$$[\text{VOCH}^+] = [\text{H}_3\text{O}^+]_0(1 - e^{-k[\text{VOC}]t}) \approx [\text{H}_3\text{O}^+]_0 [\text{VOC}] k t \quad (3.1.2)$$

Primary and product ions are then detected by the MS in the usual way. The great advantage of this method, however, is that fragmentation of the product ions is very much reduced so the mass spectra produced are much easier to interpret and are more straightforward to quantify.

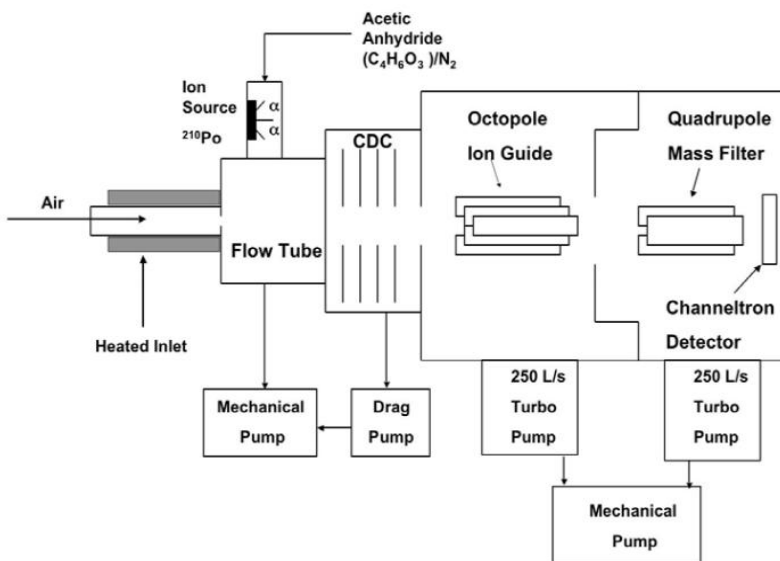


Figure 3.2: A rough sketch of NI-PTRM mass spectrometry.

The typical apparatus consists of three parts, figure: The ion source where ions are produced by a hollow cathode discharge using water vapor as the molecular source of ions; the drift tube where proton transfer reactions to the trace constituents in the air occur; and finally the ion detector which provides sensitive detection characteristic of the molecules of interest of mass selected ions .

3.2 Ion-neutral reaction Kinetics

Chemical kinetics, also known as reaction kinetics, is the study of rates of chemical processes. Chemical kinetics includes investigations of how different experimental conditions can influence the speed of a chemical reaction and yield information about the reaction's mechanism and transition states, as well as the construction of mathematical models that can describe the characteristics of a chemical reaction. In 1864, Peter Waage and Cato Guldberg pioneered the development of chemical kinetics by formulating the law of mass action, which states that the speed of a chemical reaction is proportional to the quantity of the reacting substances [10].

3.2.1 Pseudo first order reaction

There are circumstances where a second order reaction might appear, in an experiment, to be first order. That is when one of the reactants in the rate equation is present in great excess over the other in the reaction mixture. Measuring a second order reaction rate with reactants A and B can be problematic: the concentrations of the two reactants must be followed simultaneously, which is more difficult; or measure one of them and calculate the other as a difference, which is less precise. A common solution for that problem is the pseudo first order approximation [11].

If either [A] or [B] remain constant as the reaction proceeds, then the reaction can be considered pseudo first order because in fact it only depends on the concentration of one reactant. If for example [B] remains constant then

$$r = k[A][B] = k'[A] \quad (3.2.1)$$

where $k' = k[B]_0$ (k' with units s^{-1}) and an expression is obtained identical to the first order expression above.

One way to obtain a pseudo first order reaction is to use a large excess of one of the reactants ($[B] \gg [A]$ would work for the previous example) so that, as the reaction progresses only a small amount of the reactant is consumed and its concentration can be considered to stay constant. . For a generic reaction:



If $[A]_0 \gg [B]_0$, then, when the reaction has run to completion, (at time = infinity),

$$[A]_{\text{inf}} = [A]_0 - 2 [B]_0 \approx [A]_0 \quad (3.2.2)$$

So [A] is approximately constant throughout the entire reaction and then the rate law becomes,

$$\frac{d[A]}{dt} = -k[A][B] = -k'[B] \quad (3.2.3)$$

Form which is effectively a first order rate equation can be obtained as follow. This rate equation has the solution

$$[A] = [A]_0 e^{-k[B]_0 t} \quad (3.2.4)$$

Note that for very small x

$$e^{-x} \approx 1 - x$$

and then

$$e^{-k[A]_0 t} \approx 1 - k[B]_0 t$$

Combining this with equation (3.2.4)

$$[A] = [A]_0(1 - k[B]_0 t) \quad (3.2.5)$$

For every concentration of produce P the concentration of consumed A is given by

$$[A] = [A]_0 - [P] \quad (3.2.6)$$

Combining equation (3.2.5) and (3.2.6), the concentration of P formed after a time t is given by

$$[P] = [A]_0[B]_0 kt \quad (3.2.7)$$

Pseudo first order reactions are sometimes used to find the rate constant of a second order reaction when one of the two components is very expensive and the other one is relatively cheap. You can use an excess of the inexpensive reagent and use a small amount of the expensive one.

3.2.2 Reaction rate constant/reaction rate coefficient

A couple of theories have been developed during the last century, Collision theory and Transitional state theory, for the calculation of reaction rate of various chemical reactions. According to collision theory a reaction take place if and only if the reactant molecules collide, the collision occurs with minimum energy, and the collision has the correct aim. This theory is based on the idea that reactant particles must collide for a reaction to occur, but only a certain fraction of the total collisions have the energy to connect effectively and cause the reactants to transform into products. This is because only a portion of the molecules have enough energy and the right orientation at the moment of impact to break any existing bonds and form new ones. The minimal amount of energy needed for this to occur is known as activation energy. Particles from different elements react with each other by releasing activation energy as they hit each other. If the elements react with each other, the collision is called successful, but if the concentration of at least one of the elements is too low, there will be fewer particles for

the other elements to react with and the reaction will happen much more slowly. As temperature increases, the average kinetic energy and speed of the molecules increases but this only slightly increases the number of collisions. The rate of the reaction increases with temperature increase because a higher fraction of the collisions overcome the activation energy[12]. The formula that concludes the collision theory and, of course, leads to the Arrhenius equation comes from three factors; the collision frequency factor that calculates the number of collisions in unit volume per unit time, the steric factor that comes from orientation and the activation energy factor that corresponds to fractions of collisions with sufficient energy and is given by:

$$K = pZ \exp\left(-\frac{E_a}{RT}\right) \quad (3.2.8)$$

where k is rate constant, p is steric factor (constant), Z is collision frequency (cm^3s^{-1}), E_a is activation energy (J), R is universal gas constant ($R= 8.3145\text{J } ^\circ\text{K}^{-1}\text{mol}^{-1}$), and T is temperature ($^\circ\text{K}$). The Arrhenius equation gives the dependence of the rate constant k of chemical reactions on the temperature T and activation energy E_a as shown below:

$$k = Ae^{-E_a/RT} \quad (3.2.9)$$

where A is the pre-exponential factor or simply the pre-factor, and R is the gas constant. The gas constant R is related to the Maxwell-Boltzmann constant K_B with the equation:

$$R=K_B N_A \quad (3.2.10)$$

where N_A is given is the Avogadro number ($N_A=6.022\times 10^{23}\text{mol}^{-1}$).

Before the development of Transitional state theory (TST), the Arrhenius rate law was widely used to determine energies for the reaction barrier. The Arrhenius equation arises from empirical observation and ignores any mechanistic considerations, such as whether one or more reactive intermediates are involved in the overall conversion of a reactant to a product [13].

Transition state theory (TST) is a theory that explains the reaction rates of elementary chemical reactions and the theory assumes a special type of chemical equilibrium (quasi-equilibrium) between reactants and activated transition state complexes[14]. According to the theory; rate of reactions are calculated by kinetic theory by considering activated complexes which lie at the saddle point of a potential energy surface, the details process of formation of the complexes are not important, and the activated complexes are

assumed to be in quasi equilibrium with the reactant molecules. Figure 3.4 below shows the transition state complexes during the progress of reaction coordinate of the reaction between HO⁻ and CH₃Br. Both the theories have provided researchers with a conceptual foundation for understanding how chemical reactions take place. Even though the theories are widely accepted, they do have their own limitations [12,13,14].

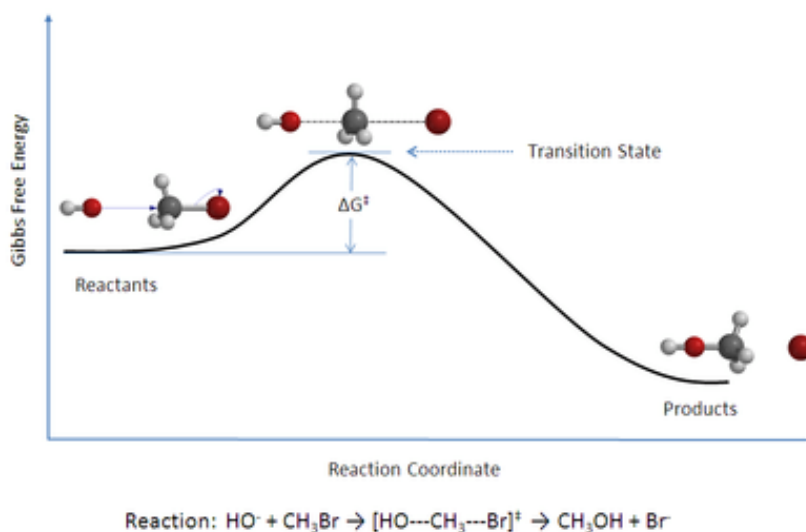


Figure 3.3: Reaction coordinates for the reaction between HO⁻ and CH₃Br.

TST has been successful in calculating the standard enthalpy of activation ($\Delta^\ddagger H$), the standard entropy of activation ($\Delta^\ddagger S$), and the standard Gibbs energy of activation ($\Delta^\ddagger G$) for a particular reaction if its rate constant has been experimentally determined. In analogy to Collision theory, the transitional state theory is concluded by Eyring equation given by:

$$k = \frac{k_B T}{h} e^{\frac{-\Delta G^\ddagger}{RT}} \quad (3.2.11)$$

where ΔG^\ddagger is the Gibbs energy of activation, k_B is Boltzmann's constant, and ($h=6.626 \times 10^{-34}$ J.s) is Planck's constant.

Because of the long range potential interaction between the reactant partners, ion-neutral molecule reaction is quite different from the case when the two reactant partners are both neutral. Because of this long range potential the collision cross section became greater than the sum of the radii of the ion and the molecule. The rate constant for ion and neutral molecule, therefore, in general, are considerably larger than those for neutral/neutral molecules. Ion-neutral molecule reactions have been an area of interest

both theoretically and experimentally since the time when Langevin's ion-induced dipole theory of ion-nonpolar molecule collision was developed in 1905 [3,13,25].

3.2.3. Neutral-neutral reaction rate constant

The reactions of ions with neutral molecules play a significant and often dominant role in the chemical and physical evolution of many gaseous plasma environments. Examples include the interstellar medium, planetary ionospheres, and industrial plasmas. Recently, and owing to the efficiency of ion-neutral reactions, ions are being used as extremely sensitive probes to the environment, allowing trace gases to be detected in extremely minute quantities. This opens up all kinds of possibilities in analytical science. The importance of these reactions is a result of the greater reactivity of ions compared to neutral species. To exploit their full potential, a full understanding of the processes involved is needed to be investigated [16].

A simplified approach for describing chemical reactions is the hard-sphere collision model, which considers a chemical reaction as a collision of rigid spheres and does not take into account any other intrinsic information about the reactants. In this case, the reaction cross section, σ (cm^2) is given by

$$\sigma = \pi b^2 \quad (3.2.12)$$

where $b = r_A + r_B$ is the sum of the radii of the molecules A and B. This model assumes that the probability of a chemical reaction to occur between molecule A and B is 1 ($P_{AB} = 1$) when the distance between the molecules is $r_{AB} = b$ and the probability for a reaction is 0 ($P_{AB}=0$) when $r_{ab} > b$. The reaction rate, $k(T)$ for the hard sphere collision model is defined as

$$K(T) = \int_0^\infty u \sigma f(u) du \quad (3.2.13)$$

where u represents the relative velocity (m/s) of the molecules A and B ($u = |u_A - u_B|$) and $f(u)$ is the Maxwell-Boltzmann velocity distribution given by

$$f(u) = 4\pi u^2 \left(\frac{\mu}{2\pi K_B T} \right)^{3/2} e^{-\frac{\mu u^2}{2K_B T}} \quad (3.2.14)$$

Introducing (3.2.12) and (3.2.14), into (3.2.13) becomes

$$K_g(T) = b^2 \sqrt{\frac{8\pi K_B T}{\mu}} \quad (3.2.15)$$

where K_B denotes the Boltzmann constant ($K_B = 1.38 \times 10^{-23} \text{J/K}$), T represents the temperature ($^{\circ}\text{K}$) and μ represents the reduced mass (kg) of the molecules A and B given by

$$\mu = \frac{m_A m_B}{m_A + m_B} \quad (3.2.16)$$

where m_A and m_B are denoting the mass of the molecule A and B respectively

3.2.4 Ion/neutral molecule reaction, theoretical models

Langevin's theory

The first theory of ion-molecule reactions was proposed by P. Langevin in 1905. The Langevin theory describes the interaction between an ion and a non-polar molecule[15]. According to this, the effective interaction potential V is given by the following expression

$$V(r) = -\frac{\alpha Q^2}{2r^4} + \frac{L^2}{2\mu r^2} \quad (3.2.17)$$

where α (Cm/V) represents the polarizability of the neutral molecule, Q is the net charge on the ion, r represents the relative distance between the ion and the molecule and L represents the classical angular momentum. The angular momentum has the form

$$L = \mu u b \quad (3.2.18)$$

With u as the relative velocity of the two particles and b (Fig 3.5.1) as the impact parameter

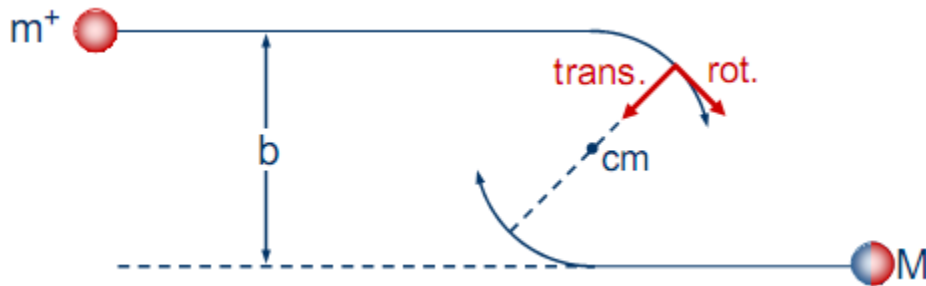


Figure 3.4: Ion-neutral molecule trajectory.

The second term in expression in equation (3.2.20) describes the repulsion between the two particles and is referred to as the centrifugal term. The relation 3.2.18 can be written in terms of the kinetic energy

$$E = \mu u^2 / 2 \quad (3.2.19)$$

and in this case, the effective potential becomes:

$$V(r) = -\frac{\alpha Q^2}{2r^4} + E \left(\frac{b}{r}\right)^2 \quad (3.2.20)$$

The Langevin potential has a maximum value along the reaction coordinate. It represents the centrifugal barrier that has to be overcome for the chemical reaction to take place, which is given by:

$$V_{max} = \frac{E^2 b^4}{2\alpha Q^2} \quad (3.2.21)$$

The critical impact parameter corresponding to V_{max} for which a chemical reaction takes place is then:

$$b_c = \left(\frac{2\alpha Q^2}{E}\right)^{1/4} \quad (3.2.22)$$

For impact parameter values $b = b_c$, the reaction probability is $P = 1$ while for $b > b_c$, the reaction does not occur and $P = 0$. Similar to the hard-sphere collision model, the reaction cross section or the Langevin cross section is defined as:

$$\sigma_L = \pi b_c^2 = \pi \left(\frac{2\alpha Q^2}{E}\right)^{1/2} \quad (3.2.23)$$

The rate constant for the Langevin model can be calculated as:

$$K_L(T) = \int_0^\infty u \sigma_L f(u) du \quad (3.2.24)$$

If one takes into account that the molecules have a Maxwell-Boltzmann distribution of velocities and equation (3.2.23) is introduced into equation (3.2.24), the expression for the Langevin rate constant is obtained to be

$$K_L = \sqrt{\frac{4\pi^2 Q^2}{\mu}} \quad (3.2.25)$$

Locked Dipole theory

According to locked dipole theory the neutral molecule will have permanent dipole μ_D shown as in Fig 3.5 below. It assumes that the ion is point charge and the molecule is point dipole [17].

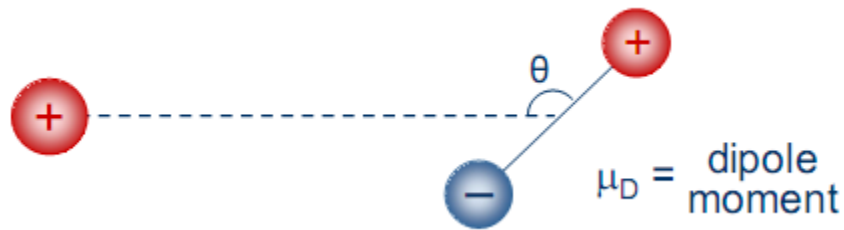


Figure 3.5: The point charge and the point dipole interaction orientation.

The effective potential in this case has an additional term arise from the interaction between the ion and permanent dipole and is given by

$$V_{eff} = \frac{L^2}{2\mu r^2} - \frac{\alpha Q^2}{2r^4} - \frac{Q\mu_D}{r^2} \cos\theta \quad (3.2.26)$$

The dipole always locked, $\theta = 0^\circ$, and $\cos\theta = 1$. The resultant rate constant for the locked dipole K_{LD} is then calculated to be:

$$K_{LD} = K_L + Q\mu_D \left(\frac{8\pi}{K_{BT}}\right)^{1/2} \quad (3.2.27)$$

Average dipole orientation theory (ADO).

The theory assumes that dipole rotation does not couple to the system rotation. The average value of orientation angle θ can be calculated as function of r [3]. The effective potential in this case is then given by:

$$V_{eff} = \frac{L^2}{2\mu r^2} - \frac{\alpha Q^2}{2r^4} - \frac{Q\mu_D}{r^2} \overline{\cos\theta(r)} \quad (3.2.28)$$

The average value of θ is obtained from the relation:

$$\bar{\theta} = \frac{\int \theta p(\theta) d\theta}{\int p(\theta) d\theta} \quad (3.2.29)$$

where $p(\theta)$ is the probability that the dipole is at an orientation of an angle θ , the corresponding cross sectional area is then given by:

$$\sigma_{ADO}(u) = \pi r_c^2 + \frac{\alpha Q^2}{r_c^2 \mu u^2} + \frac{2\pi Q\mu_D}{r_c} \overline{\cos\theta(r_c)} \quad (3.2.30)$$

r_c is ion-dipole separation at which the potential attains its maximum value. The resultant reaction rate constant for this theory is then obtained by integration of

$$K_{ADO} = \int u \sigma_{ADO} f(u) du \quad (3.2.31)$$

This gives the following result, where C is dipole locking constant. Dipole locking constant refers to the extent to which a dipole orients itself with the incoming charge and may vary between zero no alignments and one locking in.

$$K_{ADO} = \left(\frac{2\pi Q}{\mu^{1/2}} \right) \left[\alpha^{1/2} + C\mu_D \left(\frac{2}{\pi K_{BT}} \right)^{1/2} \right] \quad (3.2.32)$$

Hard Sphere Average dipole orientation (HSA) Theory

Fig 3.6 illustrates three different types of collisions between a neutral molecule and an idealized spherical cluster. If the cluster is neutral, Fig 3.6a, the molecule collides if the impact parameter is smaller than b_g , which defines the hard-sphere cross section:

If the radius of a charged cluster is smaller than the ADO capture radius, Fig 3.6b, the collision cross section can be described by ADO theory. If the radius of a charged cluster, however, is larger than the ADO capture radius, Fig 3.6c, a neutral molecule may be deflected sufficiently to collide with the cluster, without being captured. We call this a hard-sphere deflection (HSD) collision. In this case, the maximum impact parameter is larger than the geometric impact parameter from Figure 3.5.4a, $b_d > b_g$. The capture radius is velocity dependent; therefore there is a contribution of ADO capture

and HSD collisions for any cluster of finite size. The contribution of ADO capture, however, will be larger for lower temperatures and smaller clusters. In order to calculate the total collision rate, we have to calculate the impact parameter $b_d(v)$ and the critical velocity v_c at which the cross section calculation changes from ADO theory to the HSD cross section. As outlined in detail before by Su and Bowers [3], the interaction of the neutral molecule and the charged cluster is described with an effective potential $V_{eff}(r)$, which accounts for the conservation of angular momentum in the system:

$$V_{eff}(r) = \frac{\mu v b^2}{2r^2} - \frac{\alpha q^2}{32\varepsilon_0 r^4 \pi^2} - \frac{c q \mu_D}{4\pi\varepsilon_0 r^2} \quad (3.2.33)$$

Here, μ is the reduced mass of the molecule and the cluster, v their relative velocity, b the impact parameter, r the distance between the center of the cluster and the center of the molecule, q the cluster charge, and ε_0 the vacuum permittivity. The neutral molecule is described by its polarizability α , its dipole moment μ_D and the dipole locking constant c introduced by Su and Bowers [3]. According to Langevin [15], the capture radius r_c is given by the two conditions $\partial V_{eff}/\partial r = 0$ and $E_r = V_{eff}$, with the total kinetic energy E_r in the system:

$$E_r = \frac{1}{2} \mu b^2 \quad (3.2.34)$$

$$\frac{\partial V_{eff}(r)}{\partial r} = 0 = -\frac{\mu v^2 b_c^2}{r_c^3} + \frac{\alpha q^2}{8\pi^2 \varepsilon_0^2 r_c^5} + \frac{c \mu_D q}{2\pi \varepsilon_0 r_c^3} \quad (3.2.35)$$

$$V_{eff}(r) = E_r = \frac{\mu v^2 b_c^2}{2r_c^2} - \frac{\alpha q^2}{32\pi^2 \varepsilon_0^2 r_c^4} - \frac{c \mu_D q}{4\pi \varepsilon_0 r_c^2} = \frac{1}{2} \mu v^2 \quad (3.2.36)$$

Equations (3.2.25) and (3.2.26) yield the capture radius r_c :

$$r_c = \sqrt[4]{\frac{\alpha q^2}{16\pi^2 \varepsilon_0^2 \mu v_c^2}} \quad (3.2.37)$$

The critical velocity v_c for the transition from the ADO to the HSD collision regime is reached if $r_c = b_g$:

$$v_c = \sqrt{\frac{\alpha q^2}{16\pi^2 \varepsilon_0^2 \mu b_g^4}} \quad (3.2.38)$$

For $v \leq v_c$, the collision rate is calculated with ADO theory

$$K_{ADO}(v) = \frac{q}{2\varepsilon_0\sqrt{\mu}} \left(\sqrt{\alpha} + \frac{c\mu_D}{\sqrt{\mu}v} \right) \quad (3.2.39)$$

In the HSD collision regime, $v > v_c$, we have to calculate b_d for which the minimum distance between the molecule and the cluster on the trajectory amounts to b_g , which allows a hard-sphere collision. In an attractive potential, the relation between b_d and b_g is given as:

$$1 - \frac{b_d^2}{b_g^2} = \frac{V(b_g)}{E_r} \quad (3.2.40)$$

We use again $V(r)$ as derived in ADO theory [4, 20] to calculate b_d as a function of v and b_g from (3.2.38), (3.2.39) and (3.2.40):

$$V(r) = -\frac{\alpha q^2}{32\pi^2\varepsilon_0^2 r^2} \quad (3.2.41)$$

$$b_d(v) = \sqrt{b_g^2 + \frac{\alpha q^2}{16\pi^2\varepsilon_0^2\mu v^2 b_g^2} + \frac{c\mu_D q}{2\pi\varepsilon_0\mu v^2}} \quad (3.2.42)$$

This translates into the hard-sphere deflection cross-section $\sigma_{HSD}(v)$ and rate constant $k_{HSD}(v)$:

$$\sigma_{HSD}(v) = \pi b_g^2 + \frac{\alpha q^2}{16\pi^2\varepsilon_0^2\mu v^2 b_g^2} + \frac{c\mu_D q}{2\varepsilon_0\mu v^2}$$

$$k_{HSD}(v) = \sigma_{HSD}(v)v = \pi v b_g^2 + \frac{\alpha q^2}{16\pi^2\varepsilon_0^2\mu v b_g^2} + \frac{c\mu_D q}{2\pi\varepsilon_0\mu v}$$

Equation (3.2.42) shows that the geometric cross-section πb_g^2 is enlarged by the deflection of the particle towards the charged cluster. The total collision rate k_{HSA} is obtained by convoluting the ADO and HSD rate constants with the Maxwell distribution $f(v)$:

$$k_{HSA} = \int_0^{v_c} k_{ADO}(v)f(v)dv + \int_{v_c}^{\infty} k_{HSD}(v)f(v)dv \quad (3.2.43)$$

$$f(v) = 4\pi v^2 \left(\frac{\mu}{2\pi k_B T} \right)^{2/3} e^{-\frac{\mu v^2}{2\pi k_B T}}$$

The principal difficulty in the usage of these models is a reasonable estimate for b_g , i.e., the size of the cluster and the neutral collision partner. Ideally, this estimate is generally applicable. We assume that the spherical cluster of composition of the form $A.X_n$ has the same density of mixture of the bulk materials as given below:

$$\rho_{mixture} = \sum \frac{m_i}{V_i} \quad (3.2.44)$$

where m_i is mass of the i^{th} component and V_i the corresponding volume occupied by the masses. The radius of the cluster r_c cluster can then be calculated from its monomer total mass as

$$r_c = \sqrt[3]{\frac{3(m_A + nm_X)}{4\pi\rho_{mixture}}} \quad (3.2.45)$$

where m_A is mass of the component A and m_X mass of the X component.

The radius of the neutral molecule r_m molecule can be derived from the viscosity of the gas

$$r_m = \frac{1}{8} \sqrt[4]{\frac{25m_X k_B T}{\pi \eta^2}} \quad (3.2.46)$$

This yields the desired value b_g

$$b_g = r_c + r_m \quad (3.2.47)$$

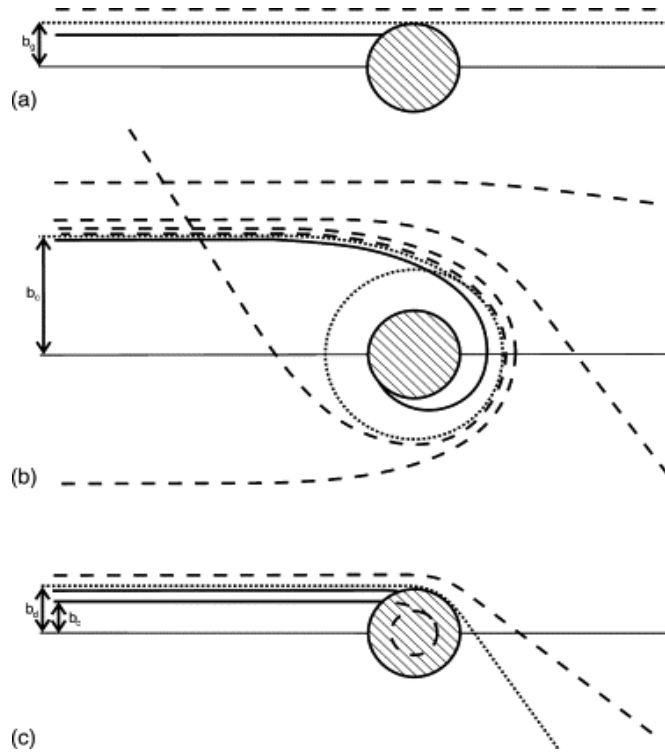


Figure 3.6: (curtesy of G. Kummerlöwe and M. Beyer, Int. J. of Mass Spec, 244 (1) p84 - 90, 2005)

Fig 3.6: Three types of collisions of a neutral molecule with a spherical cluster: (a) the cluster is also neutral. The trajectory of the molecule is linear; a collision occurs if the impact parameter b is smaller than b_g . (b) the cluster is charged and smaller than the sphere defined by the classical capture radius from ADO theory. b_c is the maximum impact parameter for which the molecule is captured. A collision occurs if $b \leq b_c$. (c) The cluster is charged and larger than the sphere described by the capture radius. If $b > b_c$, the molecule is not captured, but still deflected by the attractive interaction. A collision occurs if the closest approach occurs at a distance smaller than b_g . The maximum impact parameter b_d corresponds to the trajectory where the closest approach equals b_g .

3.3 Gas phase ion thermochemistry

In thermodynamics and physical chemistry, thermochemistry is the study of the energy evolved or absorbed in chemical reactions and any physical transformations, such as melting and boiling. Thermochemistry, generally, is concerned with the energy exchange accompanying transformations, such as mixing, phase transitions, chemical reactions, and including calculations of such quantities as the heat capacity, heat of combustion, heat of formation, enthalpy, and free energy [13].

Gibbs free energy

A spontaneous process is the time-evolution of a system in which it releases free energy, often as heat, and moves to a lower, more thermodynamically stable, energy state. The sign convention of changes in free energy follows the general convention for thermodynamic measurements, in which a release of free energy from the system corresponds to a negative change in free energy, but a positive change for the surroundings [19].

A spontaneous process is capable of proceeding in a given direction, as written or described, without needing to be driven by an outside source of energy. The term is used to refer to macro processes in which entropy increases; such as a smell diffusing in a room, ice melting in lukewarm water, salt dissolving in water, and iron rusting

The standard Gibbs free energy of a compound is the change of Gibbs free energy that accompanies the formation of 1 mole of that substance from its component elements, at their standard states (the most stable form of the element at 25 degrees Celsius and 100 kilopascals). Its symbol is ΔG .

All elements in their standard states (oxygen gas, graphite, etc.) have 0 standard Gibbs free energy change of formation, as there is no change involved.

$$\Delta_r G = \Delta_r G^\circ + RT \ln Q_r; Q_r \text{ is the reaction quotient.}$$

At equilibrium, $\Delta_r G = 0$ and $Q_r = K$ so the equation becomes $\Delta_r G^\circ = -RT \ln K$; K is the equilibrium constant.

Gas phase acidity

Gas phase acidity of a molecule AH , $\Delta_{\text{acid}}G (AH)$, is the Gibbs free energy change of the reaction:

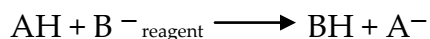


The enthalpy change of this reaction, $\Delta_{\text{acid}}H$ is the proton affinity of the anion. The Gibbs free energy change of the reaction:



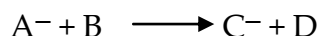
is called the relative acidity of species AH and BH [2].

The basis of this technique is selective ionization of acidic species through the transfer of a proton to the conjugate anion of a weaker acid and the subsequent detection of A^- via mass spectrometry;



The ionization scheme requires that the analyte be a stronger gas phase acid than the acidic form of the reagent ion.

Acidity determinations are based on equilibrium constants for ion/molecule reactions:



since the equilibrium constant:

$$K_{\text{eq}} = [C^-] [D] / [A^-] [B] \quad (3.3.28)$$

directly gives a value for the gibbs free energy change associated with the reaction

$$RT \ln(K_{\text{eq}}) = \Delta G = \Delta H - T \Delta S \quad (3.3.29)$$

To determine enthalpy change of these reactions, values for the entropy changes of reaction must be obtained through measurements of the equilibrium constant as a function of temperature (Van't Hoff plot) or through statistical mechanical estimations. In most studies published, change in entropy is usually small since measurements were made at single temperatures. Since we are determining the ratio of the two ion species in the presence of the neutral, we can determine the equilibrium constant and therefore ΔG directly [19]. Now, in the next chapter, we discuss on important related literatures and results obtained.

Hopping that you have grasped much detail information about theoretical background of this work, the next chapter is continued to provide the method used.

Chapter four

Methodology

The methodology of the study, in general is, the use of theoretical models as an exploration tool for the achievements of the stated objectives. We applied the hard sphere average dipole orientation HSA and the Average dipole orientation ADO models. In the use of these models we have done a computational work which include task of developing program. The program was made in such a way that it can compute NI-PTRs rate constants and the change in Gibbs free energy associated to the reaction. In the computation of this thermodynamic quantity we use pseudo first approximation as the application NI-PTR MS follows it. The program skeleton is follow, Fig 2.3.2, showing the sequence of tasks done by the program as it executed. Simpson 3/8 was used as numerical integration of the integrand function.

The expression for the K_{HSA} does not go directly into the program code. The upper limit of integration for the second term is not an appropriate number, the ambiguity that comes because of the upper limit, the infinity. There for a rearrangement was made to the expression to remove this problem. Accordingly the corresponding expression as equation 4.0.1 was obtained (see Appendix A).

The program's code was in ForTran95 (see Appendix B) as the software with its full package and relatively good capacity cluster of 4TB installed at statistical and computational physics lab in physics department, on which we run the program. The processing speed of the cluster is 3GHz with 16 quad cores of 6MB cash megabit per quad core. The input data were the constants with which the reagent ion and the neutral molecule are determined. The reagent ion is determined by its charge, molecular mass, and density. The neutral molecule is determined by its dipole moment, polarizability, dipole locking constant, molecular mass, and density. Dipole locking constant was taken to be one in all cases because literature values, corresponding to each molecule, couldn't be obtained. The value one is chosen expecting that the computed results should be greater relative to the literature.

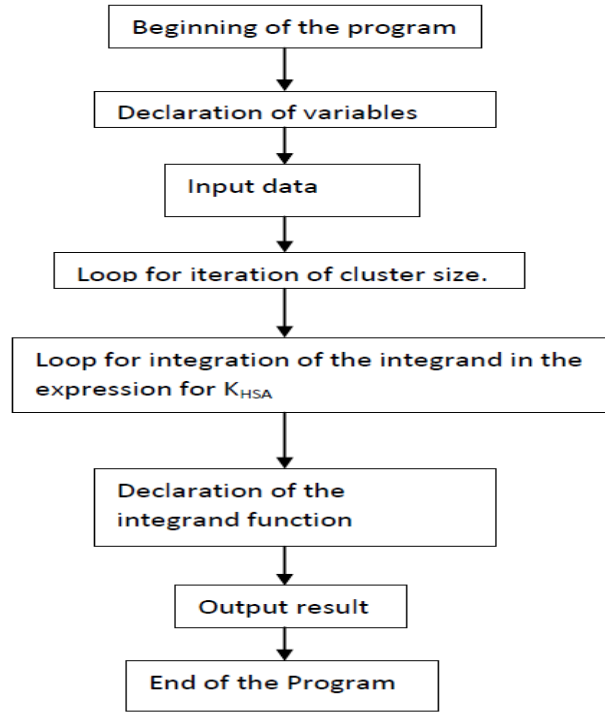


Figure 4.1: the program skeleton

$$K_{HSA} = k_1 \int_n^1 \sqrt{\ln(1/v)} dv + k_2(1 - n) + k_3(n - n \log n) + n(k_4 + k_5) \quad (4.0.1)$$

where $n = e^{-\frac{\mu v_c^2}{2k_B T}}$, $k_1 = \frac{q}{\varepsilon_0} \sqrt{\frac{\alpha}{\pi \mu}}$, $k_2 = \frac{c \mu_D q}{\varepsilon_0} \sqrt{\frac{1}{2\pi \mu k_B T}}$, $k_3 = 4\pi b_g^2 \left(\frac{\mu}{2\pi k_B T}\right)^{2/3}$,

$$k_4 = (0.5)^{5/2} \left(\frac{1}{\pi}\right)^{3/2} \frac{\alpha q^2}{\varepsilon_0^2 b_g^2} \sqrt{\frac{1}{\mu k_B T}}, \quad \text{and} \quad k_5 = \frac{c \mu_D q}{\varepsilon_0} \sqrt{\frac{1}{2\pi \mu k_B T}}$$

The following relations were used for SI unit conversion.

1. 1amu=1.667x10⁻²⁷Kg, amu-Atomic Mass Unit
2. 1D (Debye) =3.33564x10⁻³⁰C.m
3. α (C.m². V⁻¹)=(4 π ε_0 /10⁶) α (A⁰³), A⁰(angstrom)=10⁻¹⁰m

Finally, data obtained from the computational work will be tabulated using xmgrace. A number of data analyses are then made with respect to the graphs. The effect of the water clustering on the kinetic and thermodynamic variables can then be interpreted in numbers of ways.

Chapter five

Results and discussion

5.1. Review of related works

5.1.1. Ion-polar molecule collision: The effect of molecular size on ion-polar molecule reaction rate constant

According to Bowers et al, average dipole orientation ADO theory is in good agreement with experiment for the calculation of ion neutral reaction rate constant. All the Langevin, zero dipole, and locked dipole are in marked disagreement. The experiment/ADO ratios are near unity suggesting that every collision leads to reaction. Important point of observation of this work is that this ratio approximately constant despite of the change in physical size and structure of the molecules. ADO is used as diagnostic tool to investigate the importance of molecular size and structure on the magnitude of reaction rate constant. They calculated the proton transfer rate from CH_5^+ to a number of alkyl chlorides for the reaction [20]



where R represents alkyl chlorides.

As to the results, table 5.1, it was indicated that the effect of molecular size on rate constant is accounted for molecular polarizability.

5.1.2. Rate estimates for collisions of ionic clusters with neutral reactant molecules

In 2005, Beyer et al, developed a new theory, hard sphere average dipole orientation HSA theory, for the calculation of reaction rate constant between ionic cluster and neutral reactant molecules. According to them, in gas phase chemistry, the collision rate between the ion and neutral reactant molecules forms the upper theoretical limit for the reaction rate constant. This rate is frequently calculated with help of average dipole orientation theory ADO [3, 4].

Proton Transfer Rate Constants ($\times 10^9 \text{ cm}^3 \text{ molecule}^{-1} \text{ sec}^{-1}$) from CH_5^+ to Alkyl Chlorides at 300°K

	Experiment	ADO	Langevin	Locked dipole	Exptl/ADO
CH_3Cl	2.60	2.41	1.40	6.21	1.08
$\text{C}_2\text{H}_5\text{Cl}$	3.02	2.66	1.61	6.74	1.13
$n\text{-C}_3\text{H}_7\text{Cl}$	3.11	2.78	1.80	6.83	1.12
CH_3CHCH_3 Cl	3.10	2.85	1.80	7.13	1.09
$n\text{-C}_4\text{H}_9\text{Cl}$	3.20	2.86	1.93	6.90	1.12
$\text{CH}_3\text{CH}_2\text{CHCH}_3$ Cl	3.14	2.85	1.93	6.88	1.10
CH_3 $\text{CH}_3\text{-C-CH}_3$ Cl	3.28	2.90	1.93	7.09	1.13
$n\text{-C}_5\text{H}_{11}\text{Cl}$	3.29	3.03	2.08	7.26	1.09
CH_3 $\text{CH}_3\text{CH}_2\text{-C-CH}_3$ Cl	3.29	3.03	2.08	7.26	1.09

Table 5.1: Comparison of ADO to the Langevin, locked dipole and the experiment

The result of this work suggested that for polarizable molecules like water, the newly developed HSA theory rate constant lie significantly closer to experimentally measured rate constants than their ADO counter parts.

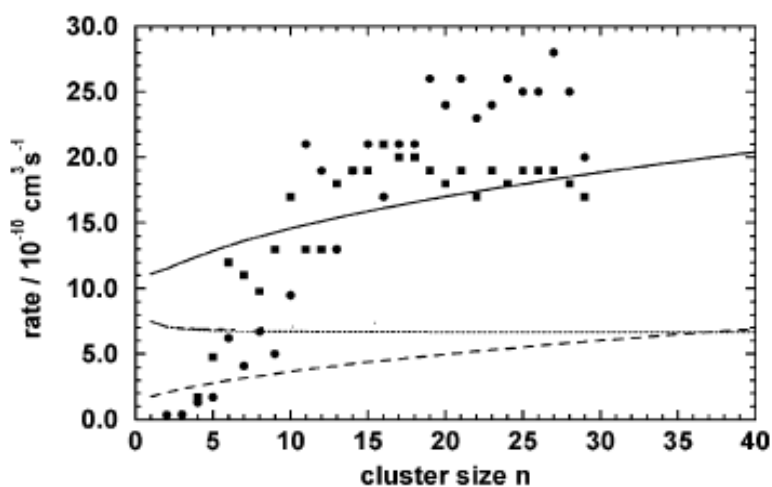
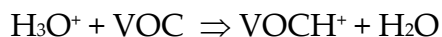


Figure 5.1: reaction rate constant for the reaction $(\text{H}_2\text{O})_n^- + \text{CO}_2 \rightarrow \text{CO}_2(\text{H}_2\text{O})_{n-m}^- + m\text{H}_2\text{O}$ computed using HSA (dot-dashed), ADO (dotted) and the purely geometric K_g (dashed) models.

5.2. Comparison of our computational results with literature

In order to test our computational capacity and accuracy, before going to our original work, we made a code and computed reaction rate constants for the reactions for which literature values are available. We compared our results for the reaction



where VOC is volatile organic compound.

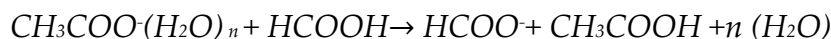
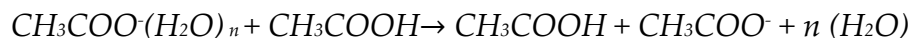
The comparison is made for ten molecules using ADO theory as in the table 5.2 below. According to this table our computational results were found to be exceeding the literature value. This comes from the fact that we used the value of the dipole locking constant to be one as there is no corresponding literature value to the molecules [26]. Dipole locking constant refers to the extent to which the dipole orients itself with the incoming charge and have the value between 0 (no alignment) and 1(locking in) [3].

					ADO($10^{-9}\text{cm}^3\text{s}^{-1}$)	
					literature	This works
Molecule	formula	Polarizability ^c	Dipole ^c moment	Molecular mass ^d		
Propyne	C ₃ H ₄	4.98	0.715	39.02	1.71	1.90
cyclobutane	C ₄ H ₆	7.19	0.121	54.05	1.69	1.81
Hexane	C ₆ H ₁₄	11.29	0.017	86.11	2.00	2.18
Toluene	C ₇ H ₈	12.90	0.343	92.06	2.12	2.21
Styrene	C ₈ H ₈	15.86	0.186	104.06	2.33	2.42
Formic acid	CH ₂ O ₂	3.05	1.144	46.01	2.02	2.17
Gloxalic acid	C ₃ H ₄ O ₂	5.25	1.276	72.02	2.00	2.18
Acetic acid	C ₂ H ₄ O ₂	4.80	1.605	60.02	2.27	2.41
keten	C ₂ H ₂ O ₂	4.04	1.493	42.01	2.21	2.33
propanal	C ₃ H ₆ O	6.13	2.748	57.05	3.44	3.57

Table 5.2: Comparison of our computational results to the available literature, (c) Taken from Zhao et al, (2004), (d) taken from CRC hand book of Chemistry and Physics 85th edition

5.3. The effect of water clustering on the reaction rate constant of acetate ion with acetic and formic acid

The effect of clustering of water, to the reagent acetate ion, on reaction rate constant was studied for the following reactions, as function of cluster size. We computed the rate constant for up hundred cluster size.



The input data

molecule	Polarizability ^a α (A ⁰³)	Dipole Moment ^a μ_D (D)	Density ^b ρ (g/cm ³)	Molecular Weight ^b M (amu)	Viscosity ^b η (mPaS)
HCOOH	3.330	1.14	1.154	46.0	1.57
CH ₃ COOH	5.11	1.74	1.049	60.05	1.22
H ₂ O	1.45	1.85	1.002	18.015	1.0

Table 5.3: The input data (a) Taken from Zhao et al, (2004), (b) taken from CRC hand book of Chemistry and Physics 85th edition

The output results were tabulated using xmgrace and shown below: Fig 5.2 for formic acid and Fig 3.3 for acetic acid.

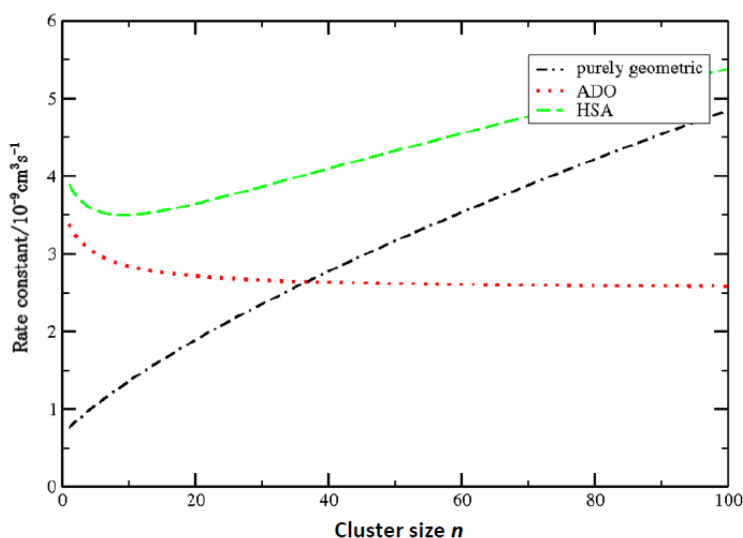


Figure 5.2: Rate constant as function of cluster size for acetic acid.

As it can easily be observed, the rate constant decrease sharply for K_{HSA} for the first 10, cluster size and starts to blow up steadily. The decreasing feature is arise due to the fact that the reduced mass increases faster on this cluster size range, Fig 5.4. This reduces the collision cross-section area which is directly, in turn, reduces the rate constant over the range.

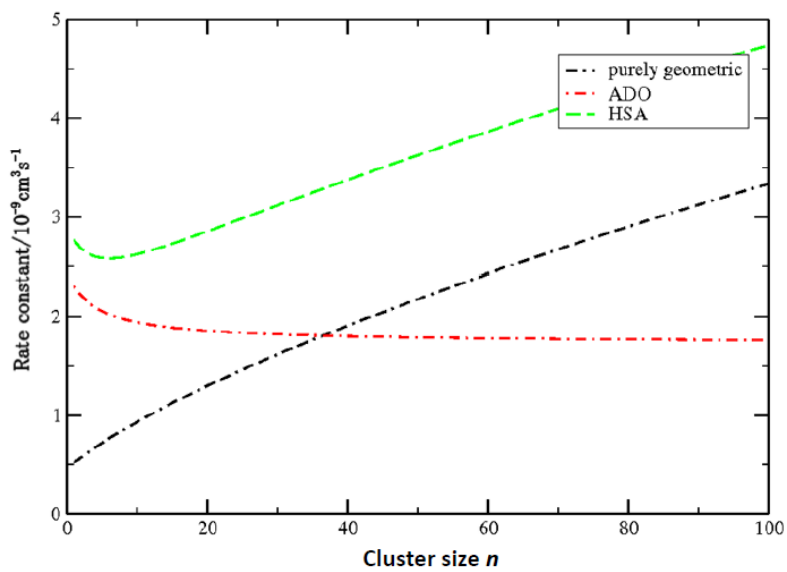


Figure 5.3: Rate constant as function of cluster size for formic acid.

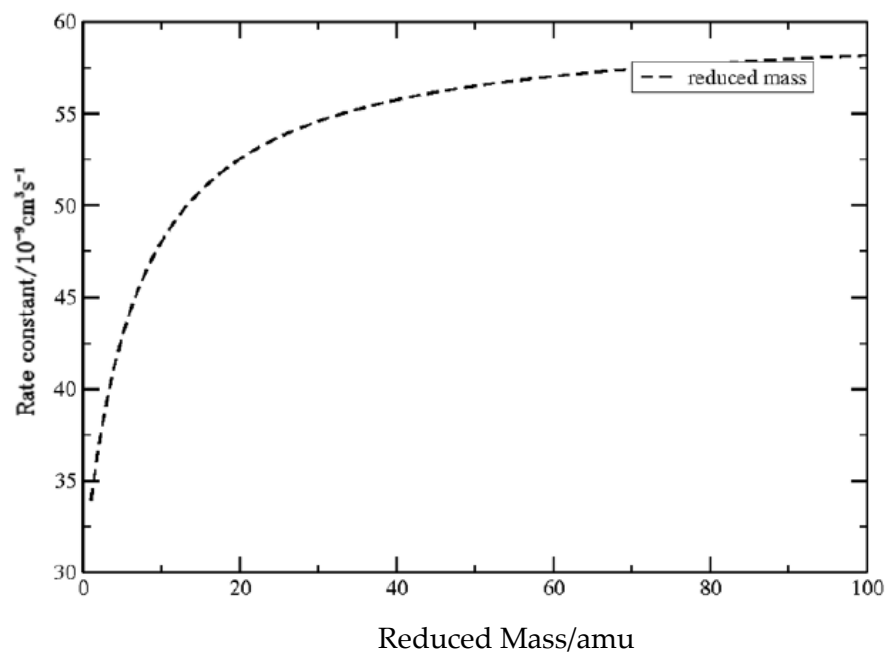


Figure 5.4: reduced mass as function of cluster size for HSA theory.

5.4. The study of the effect of molecular size and structure on the magnitude of reaction rate constant

The study of molecular size and structure on the magnitude of proton transfer rate constant of H^+ from R to CH_3COO^- . Where R is the alkyl chlorides CH_3Cl , C_2H_3Cl , $n-C_3H_7Cl$, $i-C_3H_7Cl$, $n-C_4H_9Cl$, $i-C_4H_9Cl$, $t-C_4H_9Cl$, $n-C_5H_{11}Cl$ [6].

This group of molecules was chosen because they have similar dipole moments but different molecular size and structural configuration. The reaction equation is given by



The investigation was made by using the HSA and ADO theories. The polarizabilities, α , dipole moment, μ_D , density, ρ , and the molecular weight M of these alkyl chlorides are as listed in the table below [3, 25].

<i>R</i> (Alkyl chlorides)	Polarizability ^a α (\AA^3)	Dipole Moment ^a μ_D (D)	Density ^b ρ (g/cm ³)	Molecular Weight ^b M (amu)
CH_3Cl Chlorometane	4.56	1.87	0.911	50.49
C_2H_3Cl Vinyl chloride	6.40	2.05	0.910	64.498
$n-C_3H_7Cl$ 1-chloro propane	8.24	2.05	0.892	78.540
$i-C_3H_7Cl$ 2-chloro propane	8.24	2.17	0.859	78.540
$n-C_4H_9Cl$ 1-chloro butane	9.81	2.05	0.840	95.570
$i-C_4H_9Cl$ 2-chloro butane	9.81	2.05	0.870	92.520
$t-C_4H_9Cl$ tetrabutyl chloride	9.81	2.13	0.840	9.520
$n-C_5H_{11}Cl$ 1-chloro pentene	11.6	2.16	0.870	106.594

Table 5.4: the polarizability α (in the cube of Angstrom), dipole moment μ_D (in Debye), density (in g/cm³) and molecular mass (in amu) of the alkali chlorides, (a) Taken from Bowers et al, (1973), (b) taken from CRC hand book of Chemistry and Physics 85th edition.

The structure of molecules is as shown below

<u>Chloromethane</u>	<u>Vinyl chloride</u>	<u>1-chloro propane</u>	<u>2-chloro propane</u>
CH ₃ -Cl	CH ₃ -CH ₂ -Cl	CH ₃ -CH ₂ -CH ₂ -Cl	CH ₃ -CH ₂ Cl-CH ₃
<u>1-chloro butane</u>	<u>2-chloro butane</u>	<u>tetra butyl chloride</u>	<u>1-chloro pentene</u>
CH ₃ -CH ₂ -CH ₂ -CH ₂ -Cl	CH ₃ -CH ₂ -CH ₂ Cl-CH ₃	$\begin{array}{c} \text{CH}_3 \\ \\ \text{CH}_3-\text{C}-\text{CH}_3 \\ \\ \text{Cl} \end{array}$	CH ₃ -CH ₂ -CH ₂ -CH ₂ -CH ₂ -Cl

Fig 5.5 below is to show the effect molecular size on rate constant which is accounted for quantitatively by the molecular polarizability, since polarizability is a measure of molecular size. As molecular size increases, from CH₃Cl, C₂H₅Cl to *n*-C₃H₇Cl, from *i*-C₃H₇Cl to *n*-C₄H₉Cl, and from *t*-C₄H₉Cl to *n*-C₅H₁₁Cl, the rate constant increases. Besides this, the table illustrates that the rate constant is not sensitive, in the case of the isomers, to molecular geometry (molecular structure). For example for the isomers *n*-C₃H₇Cl, *i*-C₃H₇Cl, and *n*-C₄H₉Cl, *i*-C₄H₉Cl, *t*-C₄H₉Cl the rate remain stable.

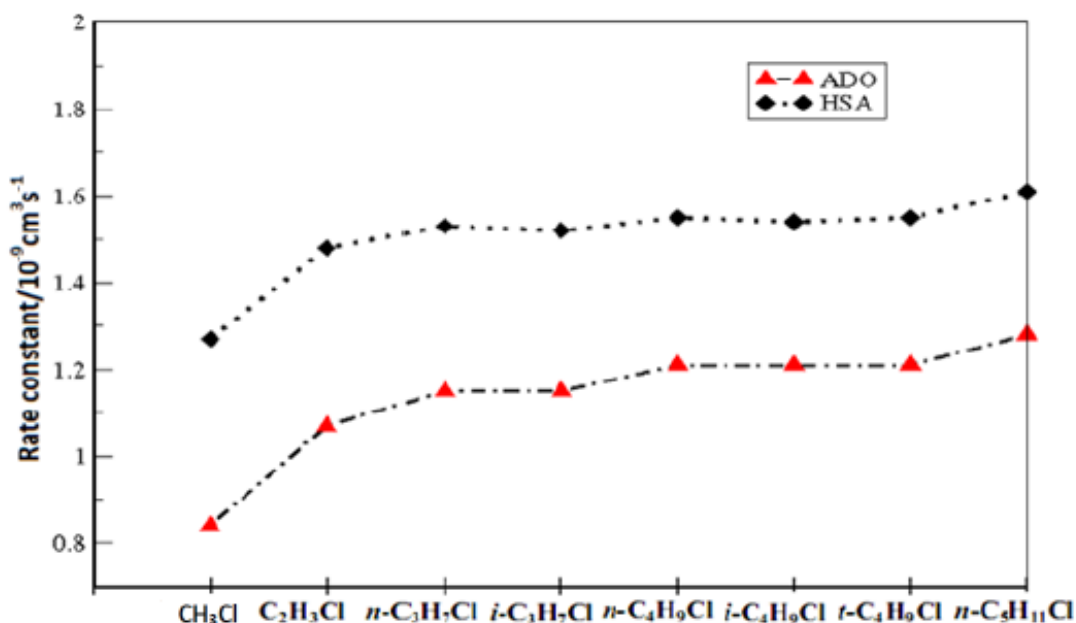
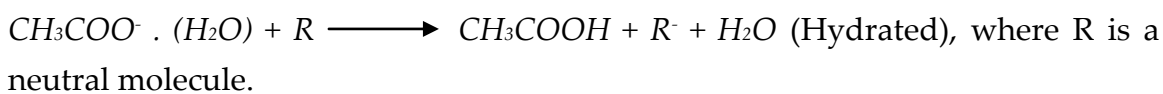


Figure 5.5: Proton transfer rate constant from alkyl chlorides, listed along the horizontal axis, to acetate ion computed by using HSA and ADO theory.

5.5. Comparison of rate constant of some the environmentally important molecules with bare and clustered/hydrated acetate ion

In this study scheme, we selected fifteen environmentally potential molecules. The selection was made in such way that molecules of wide range of dipole moment and polarizability are considered. The effect of water clustering to the reagent acetate ion on the negative ion proton transferee reaction (NI-PTR) rate constant is studied using the hard sphere average dipole orientation theory (HSA) and average dipole orientation theory (ADO). The reaction equations for this study are as given below.



The polarizabilities, α , dipole moment, μ_D , density, ρ , and the molecular weight M of these alkyl chlorides are as listed in the table below.

Molecule(R)	Formula	Polarizability ^c α (Å ⁰³)	Dipole Moment ^c μ_D (D)	Density ^d ρ (g/cm ³)	Molecular Weight ^d M (amu)
Acrylic acid	C ₃ H ₄ O ₂	5.25	1.276	1.051	72.062
Glyoxal	C ₂ H ₂ O ₂	4.71	0.004	1.140	58.036
Acetic acid	C ₂ H ₄ O ₂	4.80	1.605	1.045	60.052
1,3-Dioxane	C ₄ H ₈ O ₂	8.33	1.984	1.029	88.106
Hydrochloric acid	HCl	2.63	1.03	1.490	36.461
Furfural	C ₅ H ₄ O ₂	10.88	4.152	1.159	86.085
Nitrous acid	HNO ₂	2.89	1.42	1.00	47.013
Benzoic acid	C ₇ H ₆ O ₂	14.33	1.915	1.266	122.122
Acetyl acetone	C ₅ H ₈ O ₂	10.36	1.485	0.957	100.117
Hydrogen iodide	HI	5.44	0.45	5.228	127.912
Nitric acid	HNO ₃	2.91	2.17	1.513	63.012
Formic acid	HCOOH	3.05	1.443	1.220	46.026
P-Benzoquinone	C ₆ H ₄ O ₂	13.58	0.002	1.318	108.095
Hydrogen Fluoride	HF	0.80	1.91	0.818	20.006
Ammonia	NH ₃	2.1	1.47	0.696	17.031

Table 5.5: the polarizability α (in the cube of Angstrom), dipole moment μ_D (in Debye), density ρ (in g/cm³) and molecular mass (in amu) of the molecules, (c) Taken from Zhao et al, (2004), (d) taken from CRC hand book of Chemistry and Physics 85th edition

Fig 5.6 and Fig 5.7 show that, for all the selected molecules, the computed rates constant are found to be small for the hydrated reagent acetate ion, in both cases of the theories. The drop in the rate constant is larger for the molecules like, Acetyl acetone, Hydrogen iodide, and nitric acid for which the dipole moments are relatively larger and which are highly polarizable. Farther more the figures indicate that rate constants are larger for such molecules.

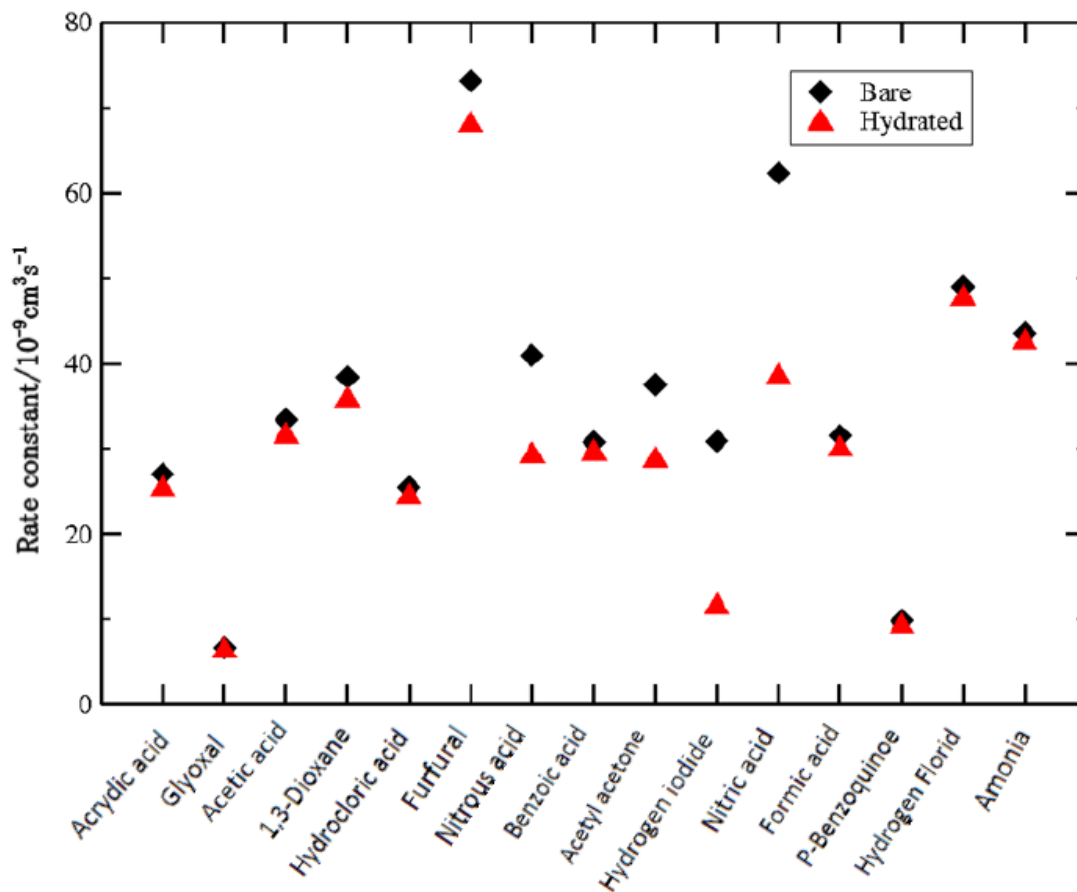


Figure 5.6: Clustering effect on the rate constant in the case of ADO theory.

5.6. Thermodynamic effect of water clustering in the negative ion proton transfer reaction (NI-PTR)

As the study of water clustering effect on the thermodynamic variables, we computed the Gibbs free energy change of the reaction of the fifteen molecules with bare and hydrated reagent acetate ion, as in section 3.3. The ΔG of the reaction [8]



$$\Delta G = -RT \ln K_{eq} \quad (5.6.1)$$

where $R(8.3145\text{J/Kmol})$ is the universal gas constant and T is the temperature at which the reaction takes place.

And from equation (1.0.4) the equilibrium constant of this reaction be comes

$$K_{eq} = \frac{[CH_3COOH][R^-]}{[CH_3COO^-][R]} \quad (5.6.2)$$

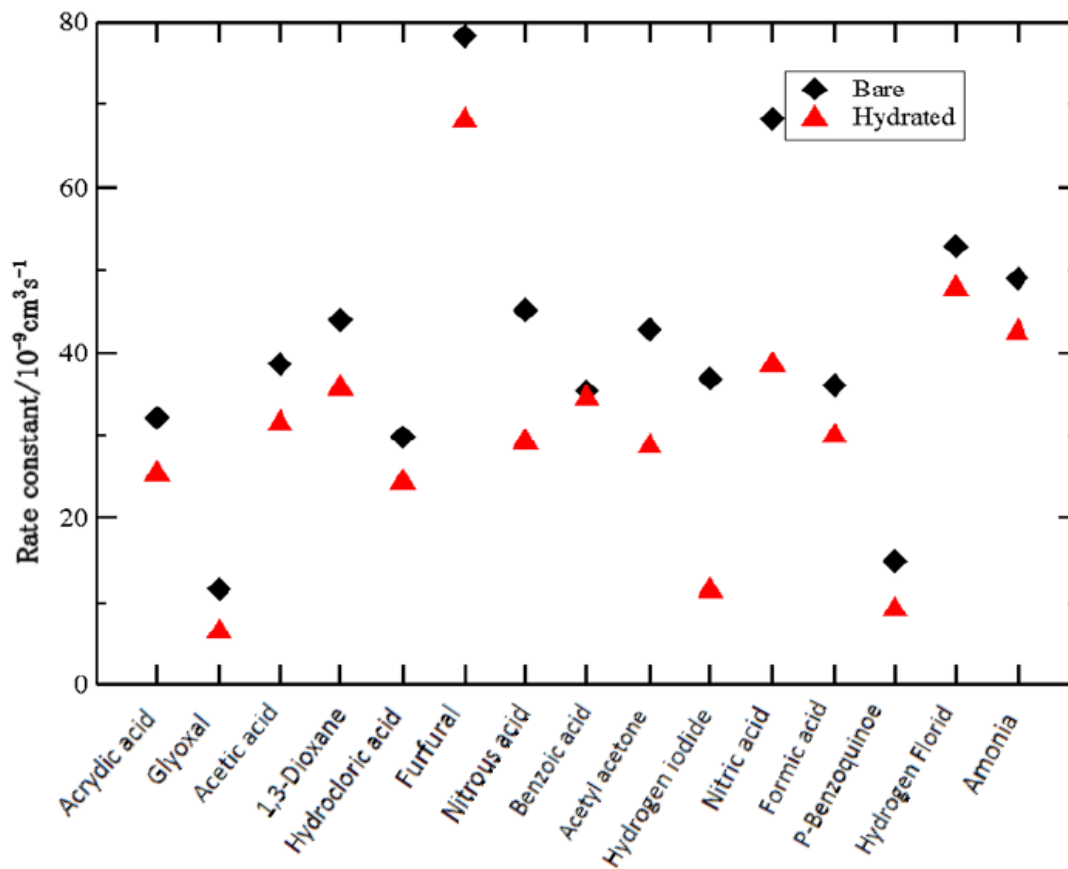


Figure 5.7: Clustering effect on the rate constant in the case of HSA theory.

Form equation (3.2.7) the concentration of the R^- produced after time t is given by

$$[R^-] = [CH_3COO^-][R]kt \quad (5.6.3)$$

where k is rate constant.

Combining equation (5.6.2) and (5.6.3), the equilibrium constant of the reaction becomes

$$K_{eq} = [R^-]kt \quad (5.6.4)$$

Here $[R^-]$ is experimental value obtained from mass spectrometer (MS) of the NI-PTR. But we can foster relations which can helps to study the effect of water clustering on the ΔG .

If we define the K_{eq}^* as the equilibrium constant for 1 second integrated reaction per the concentration of the product ion produced per second in $10^{-9}cm^3$ of volume, to be

$$K_{eq}^* = \frac{K_{eq}}{[R^-]t} \quad (5.6.5)$$

Then the corresponding ΔG^* is given by

$$\Delta G^* = -RT\ln(K_{eq}^*) \quad (5.6.6)$$

Equation 5.6.6 does not give exactly the Gibbs free energy of the reactions, but helps us to understand the effect.

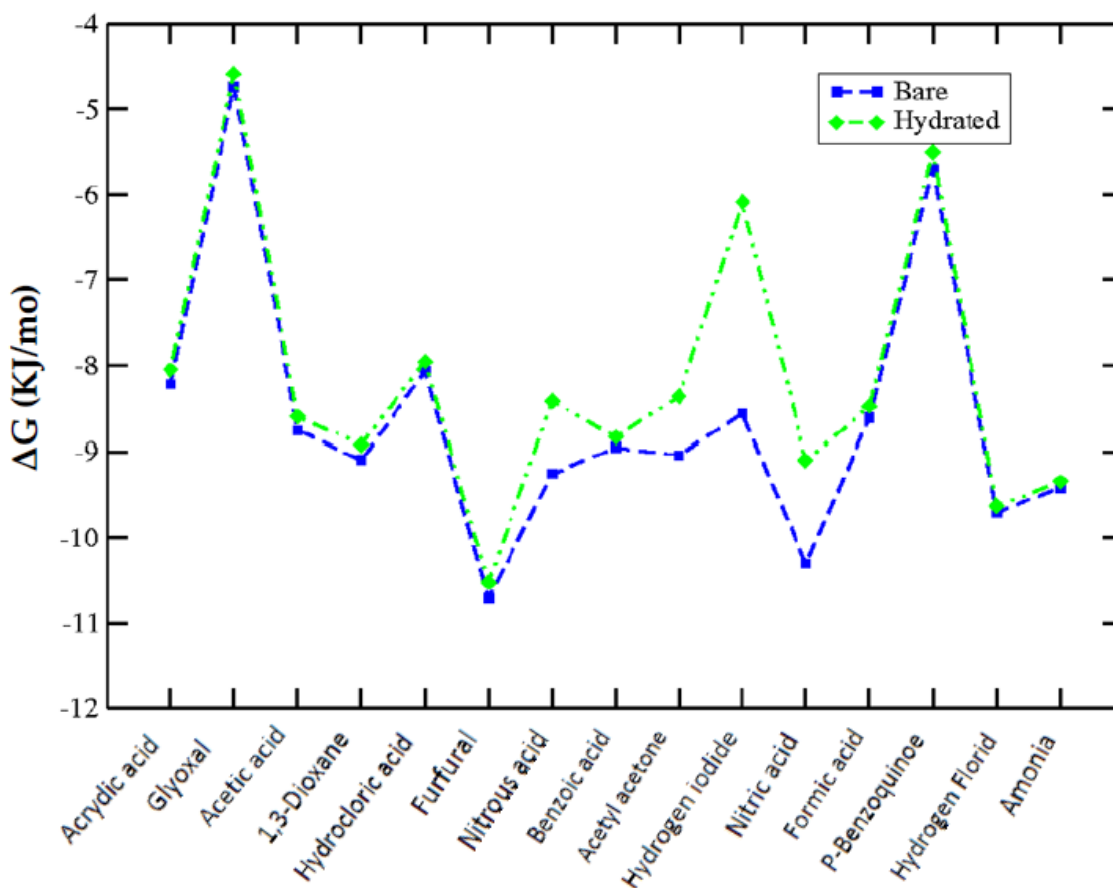


Figure 5.8: cluttering effect on Gibbs free energy change in the case of ADO theory.

Fig 5.8 and Fig 5.9 show, in contrary, for all the molecules the computed ΔG^* tend to be greater for the clustered reagent acetate ion in both cases of the theories. The increase in the results was found to be greater for the molecules like, Acetyl acetone, Hydrogen iodide, and nitric acid for which the dipole moments are relatively larger and which are highly polarizable. Farther more the figures indicate that ΔG^* are larger for such molecules. The clustering effect on the actual computation of ΔG will then be in the same way.

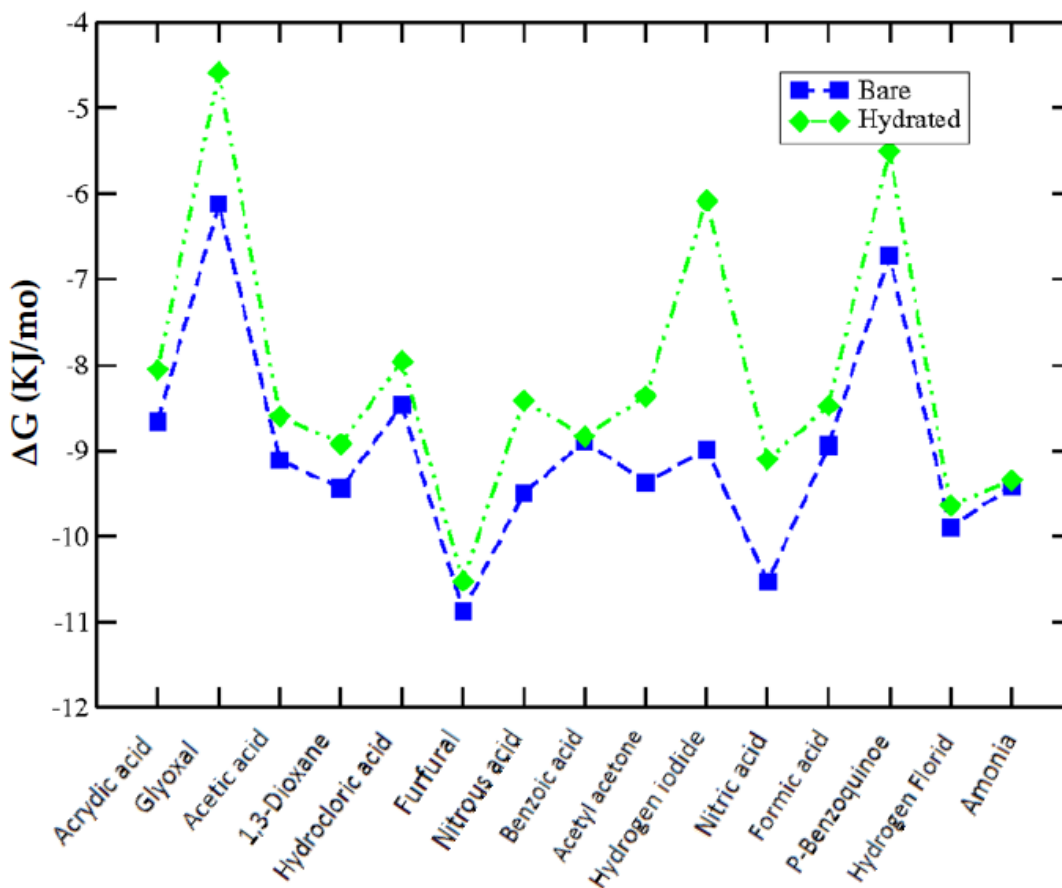


Figure 5.9: cluttering effect on Gibbs free energy change in the case of HSA theory

Chapter six

Conclusion

As it can easily be observed, the rate constant K_{HSA} decrease for the first 10 cluster size and starts to blow up steadily. The decreasing feature is arise due to the fact that the reduced mass increases faster, the dominant effect, on this cluster size range. This reduces the collision cross-section area which , in turn, reduces the rate constant over the range.

K_{HSA} always lie upper with respect to both K_g and K_{ADO} because of the additional terms in the expression of collision cross-section area.

In the investigation of the effect of molecular size and structure on the NI-PTRs rate constant, it was found that rate constant rise as molecular size enlarges and became none sensitive to molecular structure. The effect of molecular size is accounted for molecular polarizability, since polarizability is a measure of the molecular size.

Rate constants are larger for molecules with larger dipole moments and with higher polarizability constant.

Clustering of water to the reagent acetate ion was observed to affect the rate constants. The computed results show that they decrease for the hydrated reagent ion. The drop in the results was found to be greater for molecules with higher dipole moments and which are highly polarizable, in both the ADO and HAS theories.

Clustering of water to the reagent acetate ion was also found to affect Gibbs free energy change of the NI-PTRs. ΔG is reduced in the case of the non-hydrate reagent ion. This in other words means that the amount of free energy extracted in the formation of 1 mole of the product at the given temperature is reduced due to the clustering when compared to the results in the case of non-hydrated reagent ion.

Appendix A

A. The integration of K_{HSA} , a and n are the same throughout the derivation.

$$k_{HSA} = \int_0^{v_c} k_{ADO}(v)f(v)dv + \int_{v_c}^{\infty} k_{HSD}(v)f(v)dv \quad \text{A.1}$$

$$\text{where } f(v) = 4\pi v^2 \left(\frac{\mu}{2\pi k_B T}\right)^{2/3} e^{-\frac{\mu v^2}{2\pi k_B T}}, \quad K_{ADO}(v) = \frac{q}{2\varepsilon_0 \sqrt{\mu}} \left(\sqrt{\alpha} + \frac{c\mu_D}{\sqrt{\mu}v}\right),$$

$$\sigma_{HSD}(v) = \pi b_g^2 + \frac{\alpha q^2}{16\pi \varepsilon_0^2 \mu v^2 b_g^2} + \frac{c\mu_D q}{2\varepsilon_0 \mu v^2}, \quad \text{and,} \quad v_c = \sqrt{\frac{\alpha q^2}{16\pi^2 \varepsilon_0^2 \mu b_g^4}}$$

Let

$$K_{HSA} = I_1 + I_2 \quad \text{A.2}$$

And let

$$I_1 = I_a + I_b$$

$$I_a = k_1 \int_0^{v_c} v^2 e^{-av^2} dv, \quad a = \frac{\mu}{2K_B T}$$

Note

$$\int_0^{x_c} x^2 e^{-ax^2} dx = -\frac{1}{2} a^{-3/2} \int_1^n \sqrt{\ln(1/t)} dt$$

$$\text{where } n = e^{-ax_c^2} = e^{-av_c^2}$$

$$I_a = k_1 \int_n^1 \sqrt{\ln(1/t)} dt, \quad k_1 = \frac{q}{\varepsilon_0} \sqrt{\frac{\alpha}{\pi \mu}}$$

$$I_b = \int_0^{v_c} v \exp(-av^2) dv$$

Note

$$\int_0^{x_c} x \exp(-ax^2) dx = \frac{1}{2a} (1 - n)$$

$$I_b = k_2 (1 - n), \quad k_2 = \frac{c\mu_D q}{\varepsilon_0} \sqrt{\frac{1}{2\pi \mu k_B T}}$$

There fore

$$I_1 = k_1 \int_n^1 \sqrt{\ln(1/t)} dt + k_2(1 - n) \quad \text{A.3}$$

Let

$$I_2 = I_c + I_d + I_e$$

Then

$$I_c = k_3 \int_{v_c}^{\infty} v^3 \exp(-av^2) dv$$

Note

$$\int_{x_c}^{\infty} x^3 e^{-ax^2} dx = \frac{1}{2a^2} \int_0^n \ln(1/t) dt$$

Then

$$I_c = k_3(n - n \ln(n)), k_3 = 4\pi b_g^2 \left(\frac{\mu}{2\pi k_B T}\right)^{2/3}$$

$$I_d = k_4 \int_{v_c}^{\infty} v \exp(-av^2) dv = nk_4, \quad k_4 = (0.5)^{5/2} \left(\frac{1}{\pi}\right)^{3/2} \frac{\alpha q^2}{\varepsilon_0^2 b_g^2} \sqrt{\frac{1}{\mu k_B T}}$$

$$I_e = k_5 \int_{v_c}^{\infty} v \exp(-av^2) dv = nk_5$$

Therefore

$$I_2 = k_3(n - n \log n) + n(k_4 + k_5) \quad \text{A.4}$$

Combining A.3, 4 together into A.2 results in

$$K_{HSA} = k_1 \int_n^1 \sqrt{\ln(1/v)} dv + k_2(1 - n) + k_3(n - n \log n) + n(k_4 + k_5)$$


```

open(1,file="input.dat",status="old")
open(2,file="barefreeG.dat",status="replace")
open(1,file="khsa.dat",status="replace")
open(2,file="mu.dat",status="replace")
open(3,file="kg.dat",status="replace")
!+++++ ITRATION OF THE CLUSTER SIZE ++++++
      do j=1, 100
      mc= amu*(60.05+j*18.01528)
      mm= 60.0*amu
      mu=(mm*mc)/(mm+mc)
      rho=(60.05+j*18.02)/(0.057244995+j*0.01801639)
      rc=((3.0*mc)/(4.0*pi*rho))**(1.0/3.0)
      !rm=((3.0*mc)/(4.0*pi*rhom))**(1.0/3.0)
      rm=0.125*((25.0*mm*boltz*t)/(pi*visco**2.0))**(1.0/4.0)
      bg= rc+rm

k1=(q/epslon)*sqrt(pol_n/(pi*mu))  k2=((q*dipol_loc*dipol_mo)/epslon)*sqrt(1.0/(2.0*pi*mu*boltz*t))
K3=(2.0**1.5)*(bg**2.0)*sqrt((pi*boltz*t)/mu)
k4 =(0.5**2.5)*((pol_n*q**2)/(epslon**2.0*bg**2.0))*sqrt(1.0/(mu*boltz*t))*(1.0/pi)**1.5
k5=((dipol_loc*dipol_mo*q)/epslon)*sqrt(1.0/(2.0*pi*mu*boltz*t))
n=exp(-((pol_n*q**2.0)/(32.0*pi*pi*epslon**2.0*boltz*t*bg**4.0)))
!+++++ LOP FOR INTEGRATIN THE FUNCTION f ++++++
      h= (1.0-n)/1E6
      sums=0
      do i=0, 999999
      V=(n+i)*h
      s=f(V)*h
      sums=sums+s
      end do
      myu=mu/amu
      kg= 1E15*1.5*(pi*bg**2.0*sqrt((8.0*boltz*t)/(pi*mu)))
      khsa=1E15*(k1*sums+k2*(1-n)+k3*(n-n*log(n))+(k4+k5)*n)

```

```

        kado=1E15*(0.5*(q/epsilon)*sqrt(pol_n/(mu))+k2)
        !print*,j,kado,khsa
!5 format (3(E16.8,4x))
! WRITE(1,5) kg, kado, khsa
        WRITE(1,*)j, kg, kado, khsa
        WRITE(2,*)j, myu
        WRITE(3,*)j,sums
        freeg1 = -r*t*log(kado)
        freeg2 = -r*t*log(khsa)
        print*, freeg1, freeg2
        write(2,*) freeg1, freeg2

end do

end program HSA

!+++++ DECLARATION OF THE FUNCTION f ++++++

        function f(V)
        implicit none
        integer, parameter :: long=selected_real_kind(15,307)
        real(long),intent(in):: V
        Real(long):: f
        f=sqrt(log(1.0/V))
        end function f

!+++++ THE END OF THE PROGRAM ++++++

```

References

1. Su, T. and M. T. Bowers (1973). "Theory of ion-polar molecule collisions. Comparison with experimental charge transfer reactions of rare gas ions to geometric isomers of difluoro benzene and dichloroethylene. *The Journal of Chemical Physics* 58(7) 3027-3037
2. Kummerlöwe, G. and M. K. Beyer (2005). "Rate estimates for collisions of ionic clusters with neutral reactant molecules." *International Journal of Mass Spectrometry* 244(2005)84-90.
3. J. Viindanoja et al. *Laboratory investigation of negative ion molecule reaction of Propionic, butyric, pyruvic, and pionic acids*, *International journal of Mass spectrometry* 194(2000)53-68
4. Ervin, K.M., *Experimental Techniques in Gas-Phase Ion Thermo chemistry*. Chemical Reviews, 2001. 101(2)391-444.
5. A. Hansel, A. Jordan, R. Holzinger, P. Prazeller W. Vogel, W. Lindinger, *Proton transfer reaction mass spectrometry: on-line trace gas analysis at ppb level*, *Int. J. of Mass Spectrom. and Ion Proc.*, 149/150, 609-619 (1995).
6. R. D. Levin and S. G. Lias, *Ionization Potential and Appearance Potential Measurements, 1971-1981*, *Nat. Stand. Ref. Data Ser., Nat. Bur. Stand. (U.S.)*, 71 (1982).
7. Siri, William, *Mass spectroscope for analysis in the low-mass range*. *Review of Scientific Instruments* (1947). 18 (8): 540-545
8. Inomata, S., ET al., *A novel discharge source of hydronium ions for proton transfers reaction ionization: design, characterization, and performance*. *Rapid Communications in Mass Spectrometry* 2006 20(6): p 1025-1029.
9. Y. Ikezoe, S. Matsuoka and A. Viggiano, *Gas Phase Ion-Molecule Reaction Rate Constants through 1986*, Maruzen Company Ltd., Tokyo, (1987).
10. Perrot, Pierrre, (1998). *A to Z of thermodynamics*, oxford university press
11. Alex.G.Harrison, *Ionization Mass spectrometry*; CRC Press, 1992, 2nd edition, PP(7-19)
12. Eric V. Anslyn and Dennis A. Dougherty. *Transition State Theory and Related Topics*. In *Modern Physical Organic Chemistry* University Science Books: 2006, PP(365-373)
13. Truhlar, D. G., Garrett, B.C., Klippenstein, S. J., *Current Status of Transition-State Theory*. *The Journal of physical chemistry* 1996, 100, PP(12771-12800)
14. P.Langevin, *Ann. Chem.Phys.* 5,245, 1905
15. R.S. Berry, S.A rice, J. Rossa, *Physical Chemistry*, Wiley, new York, 1980, 1st edition, 1141
16. T.F.Moran and W.H.Hamill. *Cross section of ion-permanent dipole reactions by mass spectrometry*. *J.Chem.Phys.* 1963,39,6

17. Munson, M.S.B.; Field, F.H. J. Am. Chem. Soc. 1966, 88, 2621-2630. *Chemical Ionization Mass Spectrometry. I. General Introduction*
18. K.M.Ervin and V.F. Deturi, J.phys.chem, 2002, 106(42)
19. Su, T. and M. T. Bowers (1973). *Theory of ion-polar molecule collisions. The effect of molecular size and structure on ion-polar molecule rate constant* 95(1973-01-01)
20. J. Zhao, R.Zhang, *proton transfere reaction between hydronium ion and velotile organic compounds*, 2004, 38

Declaration

This thesis is my original work, has not been presented for a degree in any other University and that all the sources of material used for the thesis have been dully acknowledged.

Name: GEMECHIS DEREJE DEGAGA

Signature:

Place and time of submission: Addis Ababa University, June 2010

This thesis has been submitted for examination with my approval as University advisor.

Name: Dr. MULUGETA BEKELE

Signature: